

THE UNIVERSITY OF MICHIGAN

**COLLEGE OF ENGINEERING
DEPARTMENT OF ENGINEERING MECHANICS
TIRE AND SUSPENSION SYSTEMS RESEARCH GROUP**

64 p.

N64 13192*

Technical Report No. 1

CODE-1

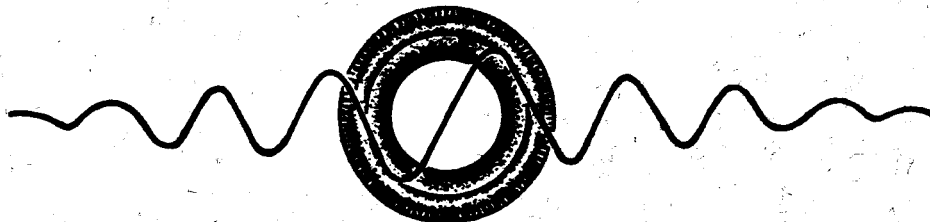
Deformation and Stress in an Inflated Aircraft Tire

NASA CR 55174

S. K. CLARK
R. N. DODGE
J. T. TIELKING
B. HERZOG

OTS PRICE

XEROX \$ *6.60 ph.*
MICROFILM \$ *2.12 mf.*



Under contract with:

**National Aeronautics and Space Administration
Grant No. NsG-344
Washington, D. C.**

Administered through:

October 1963

5726005
~~THE UNIVERSITY OF MICHIGAN~~

U., Ann Arbor

② COLLEGE OF ENGINEERING

Department of Engineering Mechanics
Tire and Suspension Systems Research Group

T ② Technical Report No. 1

T DEFORMATION AND STRESS IN AN INFLATED AIRCRAFT TIRE

S. K. Clark,
R. N. Dodge,
J. T. Tielking, and
B. Herzog

Oct. 1963 640 refs

ORA Project 05608

under contract with:

②
NATIONAL AERONAUTICS AND SPACE ADMINISTRATION
(NASA GRANT NO. NSG-344)
WASHINGTON, D.C.

administered through:

OFFICE OF RESEARCH ADMINISTRATION ANN ARBOR

October 1963

(NASA CR-55174)
Rept. 05608-2-T
CRS: 86.60 ph, 82.12 mf

The work described in this report was sponsored by The National Aeronautics and Space Administration under Grant NsG-344. It has drawn heavily on previous work jointly sponsored by:

FIRESTONE TIRE AND RUBBER COMPANY

GENERAL TIRE AND RUBBER COMPANY

B. F. GOODRICH TIRE COMPANY

GOODYEAR TIRE AND RUBBER COMPANY

UNITED STATES RUBBER COMPANY

TABLE OF CONTENTS

	Page
LIST OF ILLUSTRATIONS	vii
NOMENCLATURE	ix
I. FORWORD	1
II. SUMMARY	3
III. REVIEW OF TOROIDAL SHELL LITERATURE	5
IV. GEOMETRY OF AXISYMMETRIC DEFORMATION OF A TOROIDAL SHELL	9
V. PRINCIPLE OF POTENTIAL ENERGY APPLIED TO AN ORTHOTROPIC TOROIDAL SHELL	19
VI. THE RITZ METHOD AS AN APPROXIMATION TO THE PRINCIPLE OF POTENTIAL ENERGY	27
VII. SUMMARY OF STUDIES ON THE ELASTIC NATURE OF CORD-RUBBER LAMINATES	33
VIII. INTERNAL STRESS ANALYSIS OF THE TOROIDAL SHELL UNDER INTERNAL PRESSURE	37
IX. DIGITAL COMPUTER PROGRAM FOR CORD LOADS, INTERPLY STRESSES, AND DEFORMATIONS DUE TO INFLATION	39
X. EXAMPLE ANALYSIS	41
ACKNOWLEDGMENTS	53
REFERENCES	55

LIST OF ILLUSTRATIONS

TABLE	Page
I. 'F' Functions for Simultaneous Equations in Coefficients a_n and b_n	32
II. Comparison Between Measured and Calculated Cord Angles	35

FIGURE	
1. Geometry of tire forming from a drum.	9
2. Toroidal shell nomenclature.	11
3. Coordinates for the geometry.	13
4. Tire displacements.	14
5. Tire geometry before and after inflation.	23
6. Input and output pages of digital computer program.	43
7. Comparison of calculated and measured inflated shapes for a 32x8.8 aircraft tire.	50
8. Photographs of a tire.	52

NOMENCLATURE

English Letters:

- A Shell surface area.
- a,b Coefficients in the Fourier series expansion of deflections.
- a_{ij} Constants associated with generalized Hooke's law.
- E_{ϕ}, E_{θ}, F Orthotropic elastic constants.
- $\bar{E}_{\phi}, \bar{E}_{\theta}, \bar{F}$ Orthotropic elastic constants.
- F_1, F_2, F_4, F_5 Coefficients appearing in the linear algebraic equations for a_n and b_n .
- h Shell thickness.
- $\bar{i}, \bar{j}, \bar{k}$ Unit vectors in Cartesian coordinates
- k_{ϕ}^*, k_{θ}^* Geometric quantities associated with bending.
- L,M Coefficients used in predicting cord load.
- $M_{\phi\phi}, M_{\theta\theta}$ Shell moments, moment per unit length of shell.
- $N_{\theta}, N_{\phi}, N_{\phi\phi}, N_{\theta\theta}$ Shell membrane forces, per unit length of shell.
- n End count, also any integer.
- \bar{n} Unit vector normal to shell surface.
- P Cord load, lb.
- p Internal pressure, psi.
- R_{11}, R_{22}, R_{12} Principal radii of curvature, and twist, respectively, of the midplane of the shell.
- r_0, r_1, r_2 Shell radii of curvature.
- \bar{r} Position vector to any point on shell surface.
- t_1, t_2 Unit tangent vectors to shell surface.
- U Elastic strain energy.
- $\bar{U}(\theta, \phi)$ Vector of shell displacement.

NOMENCLATURE (Continued)

- \bar{u} Membrane contribution to vector of shell displacement.
 \bar{u}' Bending contribution to vector of shell displacement.
 u, w Shell displacement.
 W Work done.
 x, y, z Cartesian coordinates.

Greek Letters:

- α Denoting meridional direction.
 α_1, α_2 Geometric quantities.
 β Local cord angle.
 $\gamma_{\phi\theta}$ Geometric quantity associated with shear.
 τ^* Geometric quantity associated with twist.
 ϵ Strain.
 λ Green, or drum, cord angle.
 ϕ Denoting meridian direction.
 Π Strain energy density.
 σ Membrane stress.
 ζ Radius of curvature.
 σ'' Interply stress.
 μ Poisson's ratio.
 Λ A geometric quantity.

NOMENCLATURE (Concluded)

Subscripts:

- ϕ, α Meridional.
- θ Circumferential.
- f Final.
- n Interger.
- b,r Rim.
- c Crown.

I. FORWARD

A detailed study of the loading of a pneumatic tire by inflation is of interest since the inflation loads provide tensile forces in the cords which enable them to carry the usual running loads imposed on the tire. In addition, stresses between plies are generated by the internal pressure. In many designs the cord loads and interply stresses so generated are not negligible, but provide a major portion of the total loading of the tire and as such are of considerable technical interest.

A second reason for a study of the process of inflating a pneumatic tire is that elastic shape changes take place during inflation. In certain instances this can be of great importance, such as in the design of wheel wells, where generally space is at a premium. There, it is desired to make the clearances between the wheel well and tire as small as practically possible, which necessitates a knowledge of the tire inflated shape.

Third, this analysis of the results of inflation in a pneumatic tire serves as a starting point which may be used for the development of techniques which can be carried over to the more difficult problems of the tire loaded against the flat surface and the running tire against the roadway.

For all these reasons, it was thought desirable to develop methods for analyzing the problem of inflation of a pneumatic tire, and at the same time attempt to produce a workable design method for the tire engineer, so that inflation effects could be readily studied.

II. SUMMARY

13192 *✓*

The principle of potential energy is applied to toroidal shell problems with particular application to internal pressure in pneumatic tires. By use of this principle, the orthotropic nature of tire materials may easily be included in the equations governing the solution. While it may be argued that integration of the differential equations of shell equilibrium represents a more direct method of solving this problem, it is nevertheless true that energy principles do provide an alternate approach which is less susceptible to difficulties involving singularities than is direct integration. These methods of solution are perhaps not the fastest in terms of computer time, but much of this disadvantage can be overcome by programming. Past work on the elastic characteristics of orthotropic laminates, such as that of Clark,¹ is brought together and correlated in such a way that the elastic response of a pneumatic tire to inflation pressure may be determined, provided that one starts with the basic characteristics which a designer must know in order to build a tire: cord properties, rubber modulus, the geometry of individual plies, number of plies in the tire carcass, and the geometry of the tire. This means that analysis of a tire due to inflation may proceed directly from the conceptual stage without lengthy intermediate calculations or experiments.

A digital computer program has been constructed which accepts the input data discussed previously and provides as output the elastic displacements of the tire in the form of the displacements of its carcass midline. From such displacements one may calculate loads in the tire cords, interply stresses between different plies of the tire, and bead forces. These cord loads and interply stresses may be calculated on a membrane basis, on a bend-

ing basis, or by utilizing both effects. Due to the well-known difficulties in obtaining significantly accurate higher derivatives from such truncated series as are used here, no attempt will be made to calculate anything other than the membrane induced cord loads and interply stresses. This is not felt to be seriously in error since in most tires bending deformations during inflation are quite small.

An example analysis is presented for a typical 32 x 8.8 Type VII aircraft tire mounted on a standard wheel and inflated to a rated pressure of 95 psi. Comparisons between calculated deflections of this tire and deflections measured from actually inflating it are quite good, and it is believed that in general it may be possible to use such an approach as this to determine the final inflated characteristics of aircraft tires.

R J T H O R

III. REVIEW OF TOROIDAL SHELL LITERATURE

It is of considerable interest to review the history of attempts to calculate the stress state and inflated shape of pneumatic tires. References 2-7 give most of the important contributions and ideas currently being used. In general, these schemes seem to fall into two categories. In the first, as exemplified by the work of Hofferberth,⁵ the entire inflation load in a tire is assumed to be carried by the cords so that the shell stresses are proportioned in such a way that their vector resultant must lie in the direction of the cord at each local point on the tire. This results in the existence of a relationship between the two shell stresses or shell forces, N_θ in the circumferential direction and N_ϕ in the meridional direction. A second relationship is obtained, usually, from the well-known shell equilibrium equation normal to the surface of the tire. This results in a set of two equations which allow the two shell forces to be determined at any point on the surface of the tire. This determination is possible only when the shape of the tire is given, so that radii of curvature may be obtained, and when the cord angle is known at every point.

The assumption that the cords carry all the load in the tire is certainly correct during the process of expanding or forming, when the surrounding rubber is essentially plastic; however, we believe there is some question concerning the assumption that the cords carry all the loads throughout the body of the cured tire, particularly at regions of relatively high cord angle with respect to a meridional plane. Also this type of analysis does not recognize the existence of stresses set up in the vicinity of the rim due to the concentrated loads which must be applied there, nor of the presence of interply stresses. In general, it is felt that this type of approach to the

cord load problem is a simple approximation of some validity, but one that does not reflect all factors inherent in the problem.

8 A second general class of approach to the tire stress problem has been to utilize, in one form or another, the equations developed for stresses in toroidal shells made from isotropic materials. Almost invariably, only the membrane solutions have been chosen for this purpose, and, of these, only the one for the complete circular torus has had much publicity. Several rather severe approximations have to be made to consider that a pneumatic tire resembles the type of structure for which this well-known shell solution is valid. For example, Ref. 8 shows that this solution, while derived in part from basic equilibrium phenomena, does not account for the fact that the deflections at the rim of the tire must vanish, nor for the fact that the pneumatic tire is a partial torus and not a complete one. For these reasons, and for a major reason to be discussed subsequently, it is felt that the membrane shell expressions, as derived for a complete isotropic torus, are not satisfactory approximations to the stresses in a pneumatic tire.

Perhaps the most complete, thorough discussion of stresses in isotropic toroidal shells available at this time is that of Ref. 9. Here, isotropic toroidal shells of circular cross section are treated from the point of view of both membrane and bending theory. It is shown there, and is well known from previous studies, that when edge forces are applied to a partial toroidal shell, as in a pneumatic tire, the influence of these edge forces may propagate some distance into the body of the tire, particularly from regions of negative Gaussian curvature. It is certain that the form of this propagation of effects of edge loads depends on the elastic nature of the materials. For example, it would be expected that this propagation would be quite different for anisotropic materials or for orthotropic materials than for isotropic materials. It has always been maintained that it would not be possible to

understand stresses and deformations in a real pneumatic tire without first understanding thoroughly the materials going into the construction of such a tire. Somehow any solution must take cognizance of the type of elastic material comprising the pneumatic tire or toroidal shell, and this is fundamentally the primary fault of pure membrane solutions.

In connection with the propagation of edge loads into the body of the tire, Clark and Field⁶ attempt to approximate cord loads and interply stresses in the vicinity of the crown by assuming that for most constructions the propagation of edge loads is such that their effect has become negligible at the crown location. To the extent that this is true, Clark and Field's paper⁶ provides a satisfactory preliminary design tool. In view of the many possible geometries of construction, it is conceivable that orthotropic structures could be designed with elastic constants proportioned so that edge loads were indeed propagated into the vicinity of the crown. In those particular cases, the expressions proposed in Ref. 6 will be inaccurate and it will be necessary for those who use this program to compare carefully its results with those obtained from the expressions of Ref. 6 in order to fully understand the types of situations for which it may be used with accuracy.

A number of attempts have been made to obtain accurate and meaningful solutions to the problem of the isotropic toroidal shell. A brief history of these may be obtained from Timoshenko⁸ and Novishilov¹¹, in which the early work of Wissler¹² is cited. A modern analysis of the problem of the partial toroidal shell is given by R. A. Clark.⁹

All these writers use as their base isotropic materials uniform throughout the shell. While results from these analyses are useful in gaining general ideas concerning the response of orthotropic shells, they are not in themselves answers to the orthotropic shell problem. The basic difficulty with all these, as well as with the orthotropic shell problem, is that, in a toroidal shell in

which the angle tangent to the meridional cross section becomes horizontal or parallel to the circumferential plane of the torus, a discontinuity arises in attempting to define the deflection of the shell surface. This discontinuity is a mathematical one in the sense that it is not possible to determine shell stresses from membrane equilibrium equations and then to work backward through the stress-strain relations and the strain displacement relations to obtain the displacements of the shell. There is thus, at present, no easy solution to the displacements of a toroidal shell considered only as a membrane. References 9, 11, and 12 all include the effects of bending so as to remove the difficulty caused by the singular nature of the deflection of the shell as a membrane. In Ref. 9, this is accomplished by asymptotic integration of the governing differential equations of equilibrium. An approximate technique yielding rather accurate results for this same problem has recently been developed and published by Dahl.¹³ This approach utilized the principle of minimum complementary energy, which was extremely convenient for the situation being treated there, namely, the toroidal pipe expansion joint in which axial loads were applied.

None of the references mentioned in this section contemplated anything other than isotropic materials, and for that reason they are not particularly applicable to the tire problem. For the most part, this is due to the difficulty of transforming any of these approaches to an approach capable of handling an orthotropic shell of noncircular cross section.

In summary, an excellent and complete background on toroidal shell problems is available for those cases in which the shell is made from isotropic materials and is of circular cross section. These solutions are useful for indicating the general form of real solutions to inflated pneumatic tires, and also useful in indicating techniques on which one might base an approach to the orthotropic problem. None of them, however, is directly applicable as it stands.

IV. GEOMETRY OF AXISYMMETRIC DEFORMATION OF A TOROIDAL SHELL

In this section, an attempt will be made to outline the geometry of the complete sequence of operations from the construction of the tire on the drum up to its most general deformation due to inflation. First, consider formation of the uncured tire lying flat on a drum, such as shown in Fig. 1, where $O-A-\bar{O}$ represents the uncured tire. Here, the cords all lie at some initial angle λ to one another. After the required number

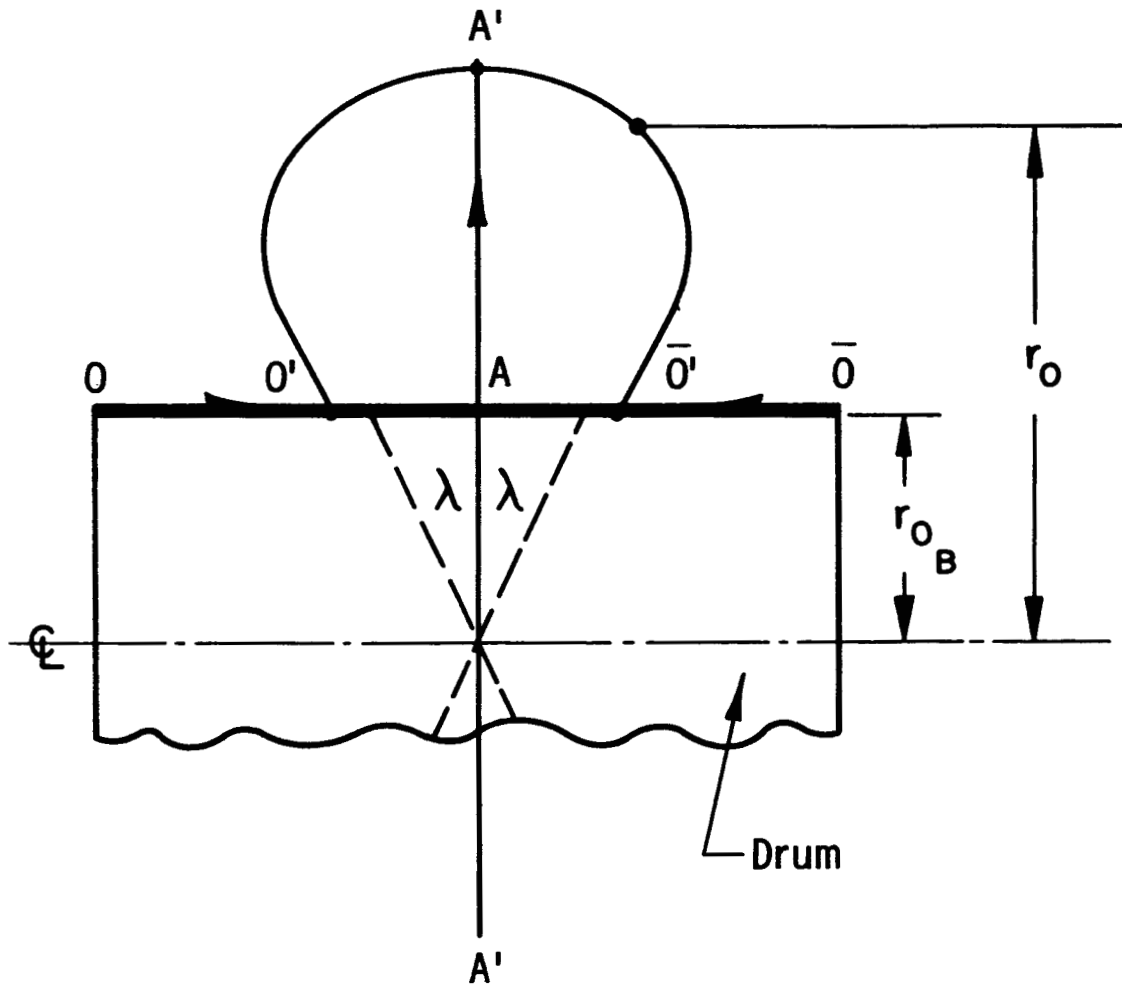


Fig. 1. Geometry of tire forming from a drum.

of plies is put on, the tire is expanded into its toroidal shape against a mould such as is also shown in Fig. 1, as the shape $O'-A'-\bar{O}'$. In the original, or unexpanded, state, all cord angles are given by λ . After expansion, various points on the drum are caused to increase in diameter so that the local cord angle, when measured from a circumferential line such as $A'A'$ in Fig. 1, is given by the symbol β where β may be approximately determined from the expression

$$\cos \beta = \frac{r_0}{r_{0B}} \cos \lambda \quad (1)$$

where r_0 is the radial dimension to a point on the midline of the tire carcass. Equation (1) is exact only if the cords are inextensible. For real textile cords a slight correction must be added. From Eq. (1), and from the symmetry of the deformation, it may be seen that the local cord angle β is a symmetric function about the crown and results in cord angles β smaller than λ at all points except at the rim. The cord angle β is a minimum at the crown, or at the position of maximum radius r_0 .

Equation (1) has appeared in various versions throughout the tire literature for many years. It represents the fundamental equation used to determine the final cord angle after forming the tire. For the present, the influence of cord extensibility is neglected in this expression, as is the possibility of the cord sliding sideways during the curing process. Equation (1) thus is an approximation to the true distribution of cord angles in the moulded tire.

Attention is next directed to geometry of deformation of the formed or expanded tire. It must be recognized at the beginning that this will be a partial torus whose cross-sectional shape is not necessarily circular. The notation here will be based on the work of Reissner and Knowles.^{14,15,16}

This is convenient since Ref. 16 will be used as a basis for constructing the elastic energy of the inflated shell or tire. In Fig. 2, a meridional cross section of a tire is

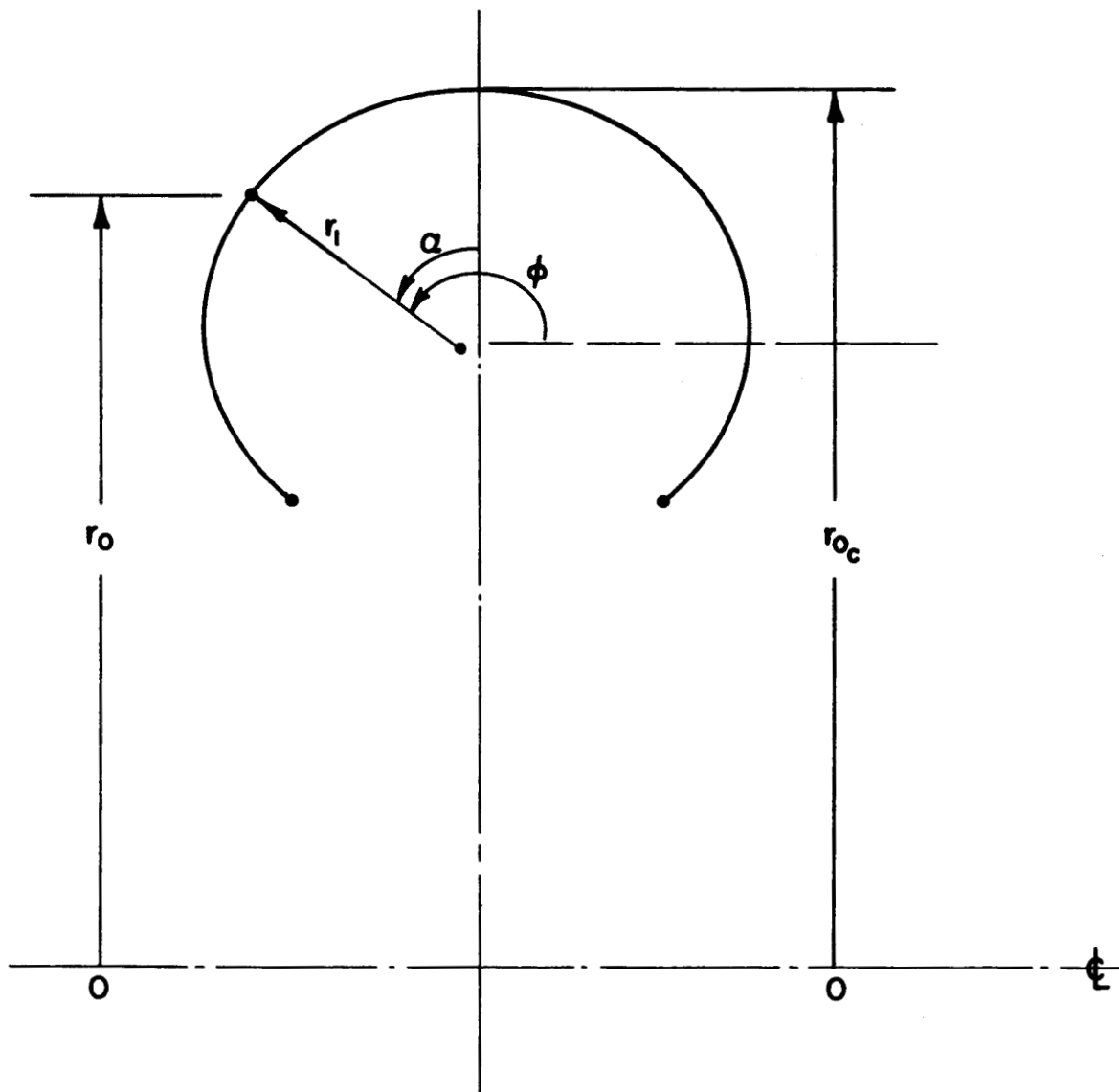


Fig. 2. Toroidal shell nomenclature.

shown giving the three fundamental dimensions used throughout the body of this report in characterizing the shape of the tire. These dimensions are r_0 , the radial dimension of any point, r_1 , the radius of curvature in the meridional

plane at that point, and the angle between the normal to the point in question and a circumferential or vertical line passing through the crown of the tire. This latter angle is denoted by the symbol α and is related to the angle ϕ shown in Fig. 2 by means of Eq. (2)

$$\alpha + \frac{\pi}{2} = \phi \quad (2)$$

The angle ϕ will occasionally be used in this report as an alternate to the angle α , since many conventional shell expressions and equations are derived on the basis of the angle ϕ rather than α . Such equations may, of course, be readily transformed into statements involving α .

A rectangular Cartesian coordinate system (Fig. 3) is now erected with the xy-plane lying in the circumferential midplane of the tire, passing through the crown. The coordinate z will be coincident with the axis of rotation OO of Fig. 2. Unit vectors \bar{i} , \bar{j} , and \bar{k} are associated with the x, y, z axes, respectively. The position vector to any point on the middle surface of the carcass may now be defined as

$$\bar{r}(\phi, \theta) = (r_0 \cos \theta) \bar{i} + (r_0 \sin \theta) \bar{j} + \left\{ - \int_{\frac{\pi}{2}}^{\phi} r_1 \sin \phi d\phi \right\} \bar{k} \quad (3)$$

provided that the $\phi = \pi/2$ point is taken as coincident with the xy-plane.

Forming derivatives, unit tangent vectors and unit normal vectors, as in Ref.

4, the principal radii of curvature can be formed as

$$\frac{1}{R_{11}} = \frac{1}{r_1^2} \frac{\partial \bar{n}}{\partial \phi} \cdot \frac{\partial \bar{r}}{\partial \phi} = \frac{r_1}{r_1^2} \left[\cos^2 \phi \cos^2 \theta + \cos^2 \phi \sin^2 \theta + \sin^2 \phi \right] = \frac{1}{r_1} \quad (4)$$

$$\frac{1}{R_{22}} = \frac{1}{r_0^2} \frac{\partial \bar{n}}{\partial \theta} \cdot \frac{\partial \bar{r}}{\partial \theta} = \frac{r_0}{r_0^2} \left[\sin^2 \theta \sin \phi + \cos^2 \theta \sin \phi \right] = \frac{1}{\left(\frac{r_0}{\sin \phi} \right)} = \frac{1}{r_2}$$

where the twist is

$$\frac{1}{R_{12}} = \frac{1}{r_1 r_0} \frac{\partial \bar{n}}{\partial \phi} \cdot \frac{\partial \bar{r}}{\partial \theta} = \frac{r_0}{r_1 r_0} \left[- \sin \theta \cos \theta \cos \phi + \sin \theta \cos \theta \cos \phi \right] = 0 \quad (5)$$

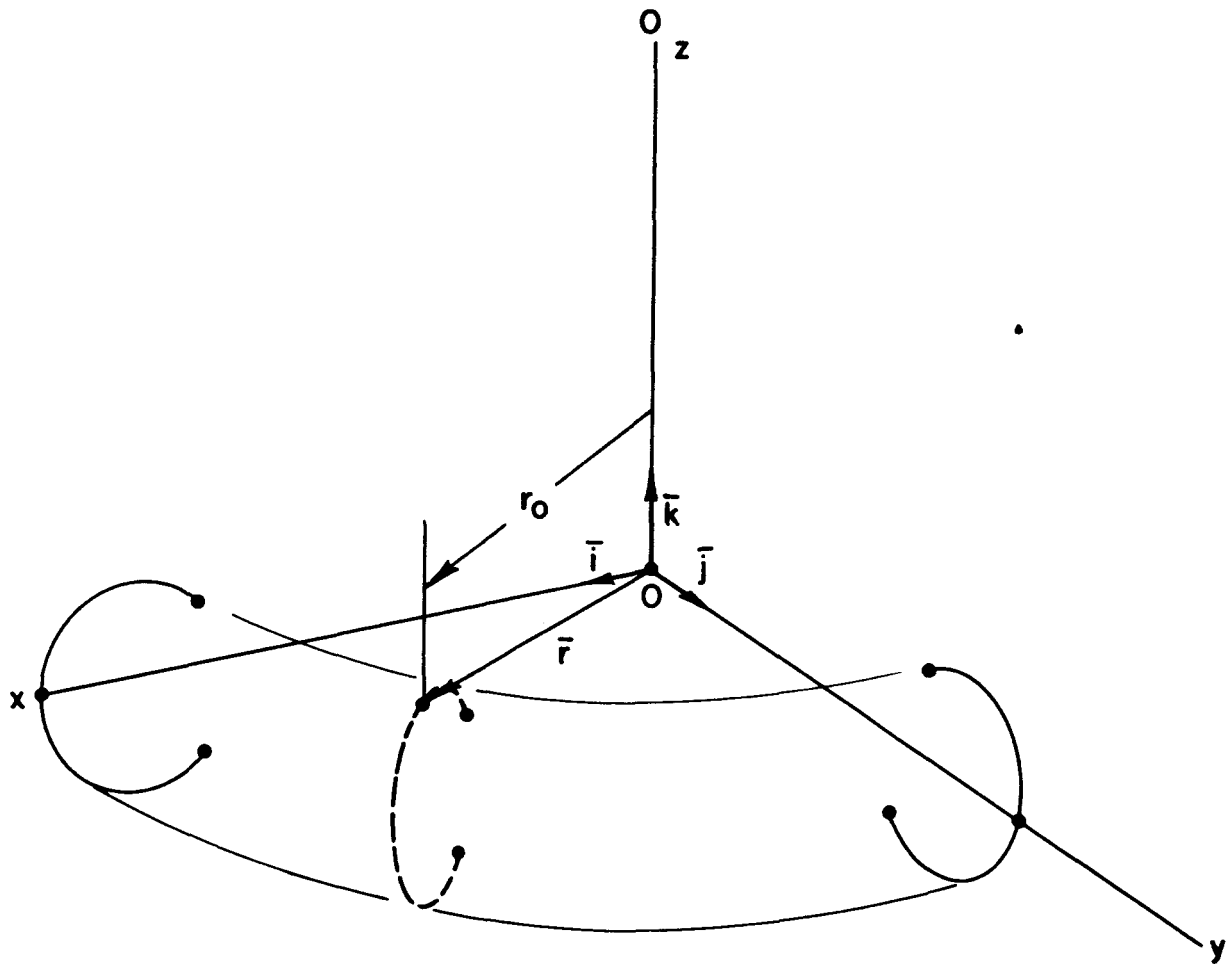


Fig. 3. Coordinates for tire geometry.

These expressions now allow the geometry of the undeformed and uninflated toroidal shell to be expressed accurately and concisely.

Consideration is now given to the geometry of deformation which may take place under axisymmetric conditions, that is, under conditions in which each meridional cross section will deform in exactly the same way independent of its circumferential position around the tire. It is now necessary to define the general vector of displacement of points on the middle surface of the carcass of the tire. This middle surface of the carcass represents a surface to which all subsequent geometry is referred and represents the surface which will

be used for calculations of shell geometry and deformation. Axisymmetric deformations may be defined in several ways, but it is convenient to presume that any point on a meridional cross section, such as point A in Fig. 4, can undergo displacements w normal to the shell middle surface and u tangential to that surface. For generality, needed in later work, we will include the displacement v , also tangent to the shell midsurface, but now lying parallel to the xy -plane of Fig. 4. In total, then, u , v , w represent displacements as shown

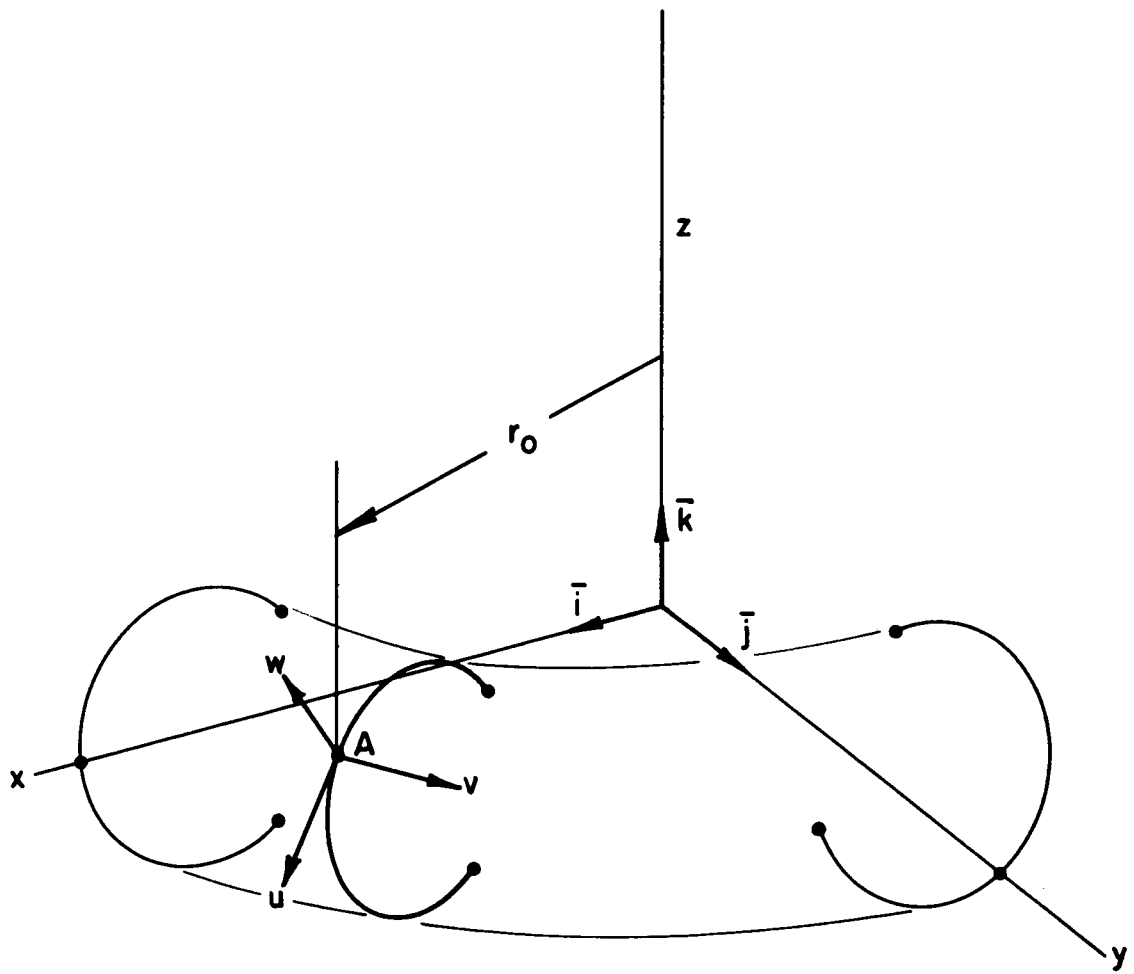


Fig. 4. Tire displacements.

in Fig. 4. In the meridional plane are u and w , v is tangent to the circle $r_0 = \text{constant}$. The vector of displacement will be called \bar{u} , so that

$$\begin{aligned}\bar{u} &= (u \cos \phi \cos \theta - v \sin \theta + w \sin \phi \cos \theta)\bar{i} \\ &+ (u \cos \phi \sin \theta + v \cos \theta + w \sin \phi \sin \theta)\bar{j} \\ &+ (-u \sin \phi + w \cos \phi)\bar{k}\end{aligned}\quad (6)$$

where, of course, \bar{u} is a displacement due to membrane effects only.

From Ref. 14,

$$\epsilon_\phi = \frac{1}{2} \gamma_{\phi\phi} = \frac{1}{\alpha_1^2} \frac{\partial \bar{r}}{\partial \phi} \cdot \frac{\partial \bar{u}}{\partial \phi} = \frac{1}{r_1} \left(\frac{\partial u}{\partial \phi} + w \right) \quad (7)$$

omitting the formation of the derivatives and the intermediate algebra. Similarly

$$\epsilon_\theta = \frac{1}{2} \gamma_{\theta\theta} = \frac{1}{\alpha_2^2} \frac{\partial \bar{r}}{\partial \theta} \cdot \frac{\partial \bar{u}}{\partial \theta} = \frac{1}{r_0} \left(u \cos \phi + w \sin \phi + \frac{\partial v}{\partial \theta} \right) \quad (8)$$

again omitting the algebra.

It is now necessary to express as a vector the bending portion of the displacement of a point some distance z from the middle surface. Consider the total displacement (membrane plus bending) to be of the form

$$\bar{U}(\phi, \theta, z) = \bar{u}(\phi, \theta) + z \left[\bar{u}'(\phi, \theta) \right] \quad (9)$$

The membrane portion $\bar{u}(\phi, \theta)$ has previously been written. The $\bar{u}'(\phi, \theta)$ portion is more difficult. Reference 14 shows that this quantity may be written

$$\bar{u}' = u'_\phi \bar{t}_1 + u'_\theta \bar{t}_2 \quad (10)$$

where

$$\begin{aligned}u'_\phi &= \frac{1}{r_1} \left(u - \frac{\partial w}{\partial \phi} \right) \\ u'_\theta &= \frac{v}{r_2} - \frac{1}{r_0} \frac{\partial w}{\partial \theta}\end{aligned}\quad (11)$$

so that, by use of Eqs. (6), \bar{u}' may be written as

$$\begin{aligned} \bar{u}' = & \left[\frac{1}{r_1} \left(u - \frac{\partial w}{\partial \phi} \right) \cos \phi \cos \theta - \left(\frac{v}{r_2} - \frac{1}{r_0} \frac{\partial w}{\partial \theta} \right) \sin \theta \right] \bar{i} \\ & + \left[\frac{1}{r_1} \left(u - \frac{\partial w}{\partial \phi} \right) \cos \phi \sin \theta + \left(\frac{v}{r_2} - \frac{1}{r_0} \frac{\partial w}{\partial \theta} \right) \cos \theta \right] \bar{j} \\ & - \left[\frac{1}{r_1} \left(u - \frac{\partial w}{\partial \phi} \right) \sin \phi \right] \bar{k} \end{aligned} \quad (12)$$

The derivatives of \bar{u}' with respect to ϕ and θ are needed. Due to their length, they will not be written out here since in the general case of asymmetric loading, u , v and w are functions of both ϕ and θ . Using these derivatives, one may obtain certain geometric quantities defined in Ref. 15 as

$$\begin{aligned} k_\phi^* &= \frac{1}{r_1^2} \left[\frac{\partial \bar{r}}{\partial \phi} \cdot \frac{\partial \bar{u}'}{\partial \phi} - \frac{1}{r_1} \frac{\partial \bar{r}}{\partial \phi} \cdot \frac{\partial \bar{u}}{\partial \phi} \right] \\ &= - \frac{1}{r_1^2} \left[\frac{u}{r_1} \frac{\partial r_1}{\partial \phi} + w - \frac{1}{r_1} \frac{\partial r_1}{\partial \phi} \frac{\partial w}{\partial \phi} + \frac{\partial^2 w}{\partial \phi^2} \right] \end{aligned} \quad (13)$$

$$\begin{aligned} k_\theta^* &= \frac{1}{r_0^2} \left[\frac{\partial \bar{r}}{\partial \theta} \cdot \frac{\partial \bar{u}'}{\partial \theta} - \frac{1}{r_2} \frac{\partial \bar{r}}{\partial \theta} \cdot \frac{\partial \bar{u}}{\partial \theta} \right] \\ &= - \left[- \frac{u}{r_0 r_1} \left(1 - \frac{r_1}{r_2} \right) \cos \phi + \frac{w}{r_0^2} + \frac{1}{r_0 r_1} \frac{\partial w}{\partial \phi} \cos \phi + \frac{1}{r_0^2} \frac{\partial^2 w}{\partial \theta^2} \right] \end{aligned}$$

Similarly, the geometric quantity $\gamma_{\phi\theta}$, defined in Ref. 15, is obtained as

$$\gamma_{\phi\theta} = \frac{1}{r_1 r_0} \left(\frac{\partial \bar{r}}{\partial \phi} \cdot \frac{\partial \bar{u}}{\partial \theta} + \frac{\partial \bar{r}}{\partial \theta} \cdot \frac{\partial \bar{u}}{\partial \phi} \right) = \frac{1}{r_0} \frac{\partial u}{\partial \theta} - \frac{v \cos \phi}{r_0} + \frac{1}{r_1} \frac{\partial v}{\partial \phi} \quad (14)$$

again omitting the intermediate algebra. From the same reference, the geometric quantity τ^* may be obtained as

$$\begin{aligned} \tau^* &= \frac{1}{r_1 r_0} \left[\left(\frac{\partial \bar{r}}{\partial \phi} \cdot \frac{\partial \bar{u}'}{\partial \theta} + \frac{\partial \bar{r}}{\partial \theta} \cdot \frac{\partial \bar{u}'}{\partial \phi} \right) - \frac{1}{r_1} \left(\frac{\partial \bar{r}}{\partial \theta} \cdot \frac{\partial \bar{u}}{\partial \phi} \right) \right. \\ &\quad \left. - \frac{1}{r_2} \left(\frac{\partial \bar{r}}{\partial \phi} \cdot \frac{\partial \bar{u}}{\partial \theta} \right) \right] \\ &= \frac{1}{r_1 r_0} \left[\frac{\partial u}{\partial \theta} \left(1 - \frac{r_1}{r_2} \right) - v \frac{r_0}{r_2^2} \frac{\partial r_2}{\partial \phi} + r_0 \left(\frac{1}{r_2} - \frac{1}{r_1} \right) \frac{\partial v}{\partial \phi} \right. \\ &\quad \left. + \frac{2}{r_0} \frac{\partial w}{\partial \theta} \left(r_1 \cos \phi \right) - 2 \frac{\partial^2 w}{\partial \phi \partial \theta} \right] \end{aligned} \quad (15)$$

These geometric quantities are sufficient to describe the possible axisymmetric deformations of the shell both from the point of view of membrane and bending effects.

V. PRINCIPLE OF POTENTIAL ENERGY APPLIED TO
AN ORTHOTROPIC TOROIDAL SHELL

In view of the general interest in deformations and shape changes of a tire upon inflation, it was felt desirable to utilize some technique from which displacement could be obtained directly. Recent work in formulating strain energy expressions for shells of revolution indicated that such expressions could be reformulated for orthotropic bodies with relatively little difficulty. For these reasons and because it seemed to lend itself conveniently to digital programming, an attempt was made to obtain solutions by means of energy techniques for the axisymmetric, partial toroidal shell under internal pressure.

Reference 16 is an attempt to utilize a rigorous geometry of deformation to construct a strain energy expression for thin elastic shells on a rational basis. This strain energy function includes certain terms not commonly used in such strain energy functions, and, as a consequence, should be somewhat more accurate for those cases where displacements are highly sensitive to secondary factors. Equation (17) of Ref. 16 will be used as the fundamental strain energy function for the tire treated as an elastic shell.

Utilizing membrane forces, membrane strains, bending moments and bending deformations as employed by Reissner and Knowles,¹⁶ the expression for strain energy density per unit area is given by Eq. (16) for the case of a shell of revolution with axisymmetric loading.

$$\Pi = \frac{1}{2} \left[N_{\phi\phi} \epsilon_{\phi} + N_{\theta\theta} \epsilon_{\theta} + M_{\phi\phi} \left(k^* + \frac{\epsilon_{\phi}}{r_1} \right) + M_{\theta\theta} \left(k^* + \frac{\epsilon_{\theta}}{r_2} \right) \right] \quad (16)$$

It is now necessary to write $N_{\phi\phi}$, $N_{\theta\theta}$, $M_{\phi\phi}$, and $M_{\theta\theta}$ in terms of the shell

displacements u , v , and w and the orthotropic elastic constants. For the two-dimensional case, Eqs. (3) and (4) of Ref. 19 give the fundamental stress-strain relations for an orthotropic body in the principal directions of elasticity. These expressions will be given here as Eqs. (17) and (18).

$$\begin{aligned}\epsilon_{\phi} &= \frac{\sigma_{\phi}}{E_{\phi}} + \frac{\sigma_{\theta}}{F} \\ \epsilon_{\theta} &= \frac{\sigma_{\phi}}{F} + \frac{\sigma_{\theta}}{E_{\theta}}\end{aligned}\quad (17)$$

$$\begin{aligned}\sigma_{\phi} &= \bar{E}_{\phi}\epsilon_{\phi} + \bar{F}\epsilon_{\theta} \\ \sigma_{\theta} &= \bar{F}\epsilon_{\phi} + \bar{E}_{\theta}\epsilon_{\theta}\end{aligned}\quad (18)$$

From Ref. 17, the shell forces are defined as

$$\begin{aligned}N_{\phi\phi} &= \int_{-\frac{h}{2}}^{\frac{h}{2}} \sigma_{\phi} \left(\frac{r_2+z}{r_2} \right) dz \\ N_{\theta\theta} &= \int_{-\frac{h}{2}}^{\frac{h}{2}} \sigma_{\theta} \left(\frac{r_1+z}{r_1} \right) dz\end{aligned}\quad (19)$$

$$\begin{aligned}M_{\phi\phi} &= \int_{-\frac{h}{2}}^{\frac{h}{2}} \sigma_{\phi} \left(\frac{r_2+z}{r_2} \right) z dz \\ M_{\theta\theta} &= \int_{-\frac{h}{2}}^{\frac{h}{2}} \sigma_{\theta} \left(\frac{r_1+z}{r_1} \right) z dz\end{aligned}\quad (20)$$

It is seen that, if the results of Eqs. (17) and (18) are substituted into Eqs. (19) and (20), a definition of the shell-membrane forces and moments per unit length may be obtained in terms of the orthotropic elastic constants and the strains in the form

$$\begin{aligned}
N_{\phi\phi} &= (\bar{E}_\phi \cdot h)\epsilon_\phi + (\bar{F} \cdot h)\epsilon_\theta + \frac{\bar{E}_\phi h^3}{12} \left(\frac{1}{r_2} - \frac{1}{r_1} \right) k_\phi^* \\
N_{\theta\theta} &= (\bar{E}_\theta \cdot h)\epsilon_\theta + (\bar{F} \cdot h)\epsilon_\phi + \frac{\bar{E}_\theta h^3}{12} \left(\frac{1}{r_1} - \frac{1}{r_2} \right) k_\theta^* \\
M_{\phi\phi} &= \bar{E}_\phi \left(\frac{h^3}{12} \right) \left(k_\phi^* + \frac{\epsilon_\phi}{r_2} \right) + \bar{F} \left(\frac{h^3}{12} \right) \left(k_\theta^* + \frac{\epsilon_\theta}{r_2} \right) \\
M_{\theta\theta} &= \bar{E}_\theta \left(\frac{h^3}{12} \right) \left(k_\theta^* + \frac{\epsilon_\theta}{r_1} \right) + \bar{F} \left(\frac{h^3}{12} \right) \left(k_\phi^* + \frac{\epsilon_\phi}{r_1} \right)
\end{aligned} \tag{21}$$

Substituting the results of Eqs. (21) into Eq. (16) gives an expression for the strain-energy density in terms of the orthotropic elastic constants and strains:

$$\begin{aligned}
\Pi &= \left[\frac{h}{2} + \frac{h^3}{24r_1r_2} \right] \left(\bar{E}_\phi \epsilon_\phi^2 + \bar{E}_\theta \epsilon_\theta^2 + 2\bar{F} \epsilon_\phi \epsilon_\theta \right) \\
&+ \frac{h^3}{24} \left[\bar{E}_\phi k_\phi^{*2} + 2\bar{F} k_\phi^* k_\theta^* + \bar{E}_\theta k_\theta^{*2} \right. \\
&\left. + \frac{2}{r_2} \left(\bar{E}_\phi k_\phi^* \epsilon_\phi + \bar{F} k_\phi^* \epsilon_\theta \right) + \frac{2}{r_1} \left(\bar{E}_\theta k_\theta^* \epsilon_\theta + \bar{F} k_\theta^* \epsilon_\phi \right) \right]
\end{aligned} \tag{22}$$

Next, Eqs. (7), (8), (10) and (11), may be substituted into Eq. (22) to obtain the strain energy in terms of the shell displacements u , v , and w . Because the number of terms involved in the strain-energy expression would become very large, the final algebraic form of this expression will not be written out here.

We turn next to the so-called work term, that is, the term involving the work done or change in potential energy of the external forces as they move through the displacements which they cause on the shell. The principal of minimum potential energy requires the variation of the work term about the equilibrium position, or deflected position. For problems in elasticity in which deflections are truly small, and for those problems which have solutions not particularly sensitive to their geometry, it has been common practice to perform the variation of the work term about the original geometry, not the

final geometry. This is, of course, much easier. In this particular case, comparison of calculated results with experiments indicate that it is not sufficient to use the original geometry for the work term. Before proceeding to that development it might be noted that strain energy should also properly be written about the final geometry. However, in all these equations, no deflection terms higher than order two are retained in order to keep the resulting algebraic equations linear. Examination of the strain energy shows that it is already of order two, based on the original geometry, and that writing it in terms of final geometry will only add higher-order terms which would be eliminated by truncation anyway. This is not the situation with the work term, which is of order one in displacements based on original geometry. It is now necessary to treat the work term on the basis of final geometry and retain in it all terms of order two or less. Figure 5 shows that r_0 and r_1 are original radii, w and u are displacements of point O to O' by means of normal and tangential directions. O has coordinates x and y , while O' has coordinates x_f and y_f .

The work term is

$$W = \int_{\text{AREA}} p \cdot w \cdot dA \quad (23)$$

where

$$dA = 2\pi r_{0f} \cdot r_{1f} d\alpha$$

Now

$$r_{0f} = r_0 + w \cos \alpha - u \sin \alpha \quad (24)$$

Calculation of r_{1f} is somewhat more complicated since it requires first the

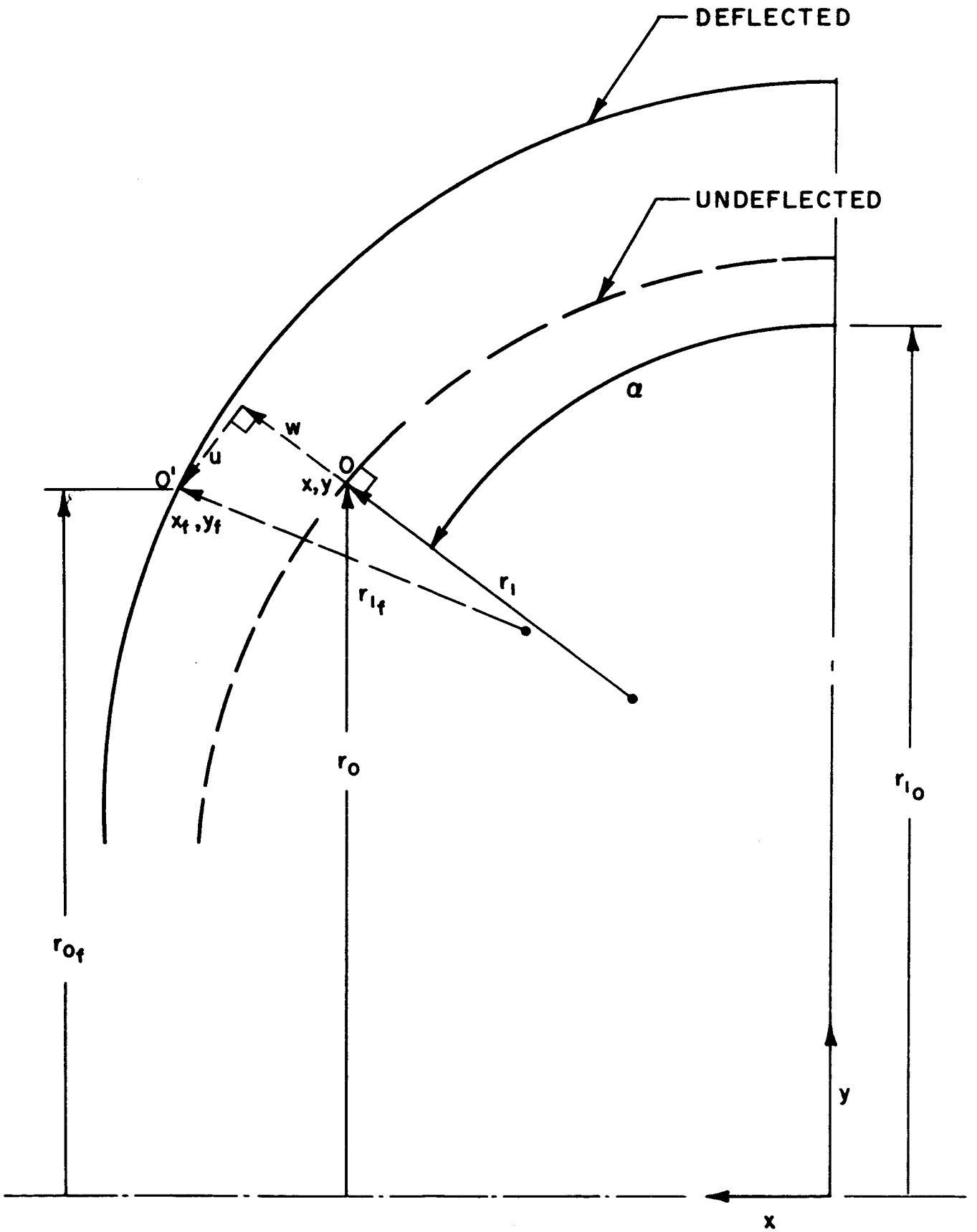


Fig. 5. Tire geometry before and after inflation.

calculation of the Cartesian coordinates of points O and O'. For O,

$$\begin{aligned} x &= \int_0^{\alpha} r_1 \cos \alpha \, d\alpha \\ y &= r_{10} - \int_0^{\alpha} r_1 \sin \alpha \, d\alpha \end{aligned} \quad (25a)$$

For O',

$$\begin{aligned} x_f &= \int_0^{\alpha} r_1 \cos \alpha \, d\alpha + w \sin \alpha + u \cos \alpha \\ y_f &= r_{10} - \int_0^{\alpha} r_1 \sin \alpha \, d\alpha + w \cos \alpha - u \sin \alpha \end{aligned} \quad (25b)$$

Reference 18, pp. 320-322, derives the expression for radius of curvature as

$$\frac{1}{\xi} = \frac{d^2 x_f / dy_f^2}{\left[1 + \left(\frac{dx_f}{dy_f} \right)^2 \right]^{3/2}} \quad (26)$$

Since x_f and y_f are linked by the parameter α , one must write

$$\frac{dx_f}{dy_f} = \frac{dx_f}{d\alpha} \cdot \frac{d\alpha}{dy_f}$$

Working out these various terms gives

$$\begin{aligned} \frac{dx_f}{d\alpha} &= r_1 \cos \alpha + w \cos \alpha - u \sin \alpha + w' \sin \alpha + u' \cos \alpha \\ \frac{d^2 x_f}{d\alpha^2} &= r_1 \sin \alpha + r_1' \cos \alpha - w \sin \alpha - u \cos \alpha + 2w' \cos \alpha \\ &\quad - 2u' \sin \alpha + w'' \sin \alpha + u'' \cos \alpha \\ \frac{dy_f}{dy_f} &= 1 = -r_1 \sin \alpha \frac{d\alpha}{dy_f} - w \sin \alpha \frac{d\alpha}{dy_f} - u \cos \alpha \frac{d\alpha}{dy_f} \\ &\quad + w' \frac{d\alpha}{dy_f} \cos \alpha - u' \frac{d\alpha}{dy_f} \sin \alpha \end{aligned}$$

from which

$$\frac{d\alpha}{dy_f} = \frac{1}{-r_1 \sin \alpha - w \sin \alpha - u \cos \alpha + w' \cos \alpha - u' \sin \alpha}$$

where primes now denote differentiation with respect to α . In addition

$$\begin{aligned}
 \frac{d}{dy_f} \left(\frac{dy_f}{dy_f} \right) &= 0 = -r_1 \sin \alpha \frac{d^2 \alpha}{dy_f^2} - r_1 \cos \alpha \left(\frac{d \alpha}{dy_f} \right)^2 \\
 &- r_1' \sin \alpha \left(\frac{d \alpha}{dy_f} \right)^2 - w \sin \alpha \frac{d^2 \alpha}{dy_f^2} - w \cos \alpha \left(\frac{d \alpha}{dy_f} \right)^2 \\
 &- w' \sin \alpha \left(\frac{d \alpha}{dy_f} \right)^2 - u \cos \alpha \frac{d^2 \alpha}{dy_f^2} + u \sin \alpha \left(\frac{d \alpha}{dy_f} \right)^2 \\
 &- u' \cos \alpha \left(\frac{d \alpha}{dy_f} \right)^2 - w' \sin \alpha \left(\frac{d \alpha}{dy_f} \right)^2 + w' \cos \alpha \frac{d^2 \alpha}{dy_f^2} \\
 &+ w'' \cos \alpha \left(\frac{d \alpha}{dy_f} \right)^2 - u' \cos \alpha \left(\frac{d \alpha}{dy_f} \right)^2 - u' \sin \alpha \frac{d^2 \alpha}{dy_f^2} \\
 &- u'' \sin \alpha \left(\frac{d \alpha}{dy_f} \right)^2
 \end{aligned}$$

Solving for $d^2 \alpha / dy_f^2$, one gets

$$\begin{aligned}
 \frac{d^2 \alpha}{dy_f^2} &= -\frac{1}{\Lambda^3} \left[r_1 \cos \alpha + r_1' \sin \alpha + w \cos \alpha + 2w' \sin \alpha \right. \\
 &\quad \left. - w'' \cos \alpha - u \sin \alpha + 2u' \cos \alpha + u'' \sin \alpha \right]
 \end{aligned}$$

where

$$\Lambda = r_1 \sin \alpha + w \sin \alpha + u \cos \alpha - w' \cos \alpha + u' \sin \alpha$$

Now the radius of curvature can be formed to give

$$\frac{1}{\zeta} = \frac{\{(r_1+w)^2 - w''(r_1+w+u') + 3u'(r_1+w) + u(u-r_1-3w'-u'') + w'(r_1+2w'+u'') + 2u'^2\}}{\{(r_1+w)^2 + u^2 + w'^2 + u'^2 + 2(r_1u'+wu'-uw')\}^{3/2}} \quad (27)$$

after considerable algebraic simplification.

In this expression, we need retain only first powers of w and u , since one w already exists in the work term. Factoring r_1^2 from both numerator and denominator and assuming small displacements and small derivatives of displacements, one may expand quantities in brackets as power series and finally

obtain

$$\zeta = r_1 \left[1 + \frac{w}{r_1} + \frac{w''}{r_1} + \frac{ur_1'}{r_1^2} - \frac{w'r_1'}{r_1^2} + \dots \right] \quad (28)$$

Thus the final radius of curvature r_{1f} is given by

$$r_{1f} = r_1 + w - \frac{w'r_1'}{r_1} + w'' + \frac{ur_1'}{r_1} \quad (29)$$

Equations (24) and (29) may now be used in Eq. (23) to compute the work term in the form

$$\begin{aligned} W &= 2\pi p \int_{-\alpha_r}^{\alpha_r} w(r_0 + w \cos \alpha - u \sin \alpha) \left[r_1 + w - \frac{w'r_1'}{r_1} + w'' + \frac{ur_1'}{r_1} \right] d\alpha \\ &= 2\pi p \int_{-\alpha_r}^{\alpha_r} \left\{ r_0 r_1 w + w^2 [r_0 + r_1 \cos \alpha] + w w'' r_0 - r_0 \frac{w w' r_1'}{r_1} \right. \\ &\quad \left. - uw \left(r_1 \sin \alpha - \frac{r_1' r_0}{r_1} \right) \right\} d\alpha \end{aligned} \quad (30)$$

This represents the work done by an internal pressure p acting inside the toroidal shell of revolution whose boundaries are at the normal angles $+\alpha_r$ and $-\alpha_r$ as measured from the crown. This expression cannot be simplified further until some decision is reached concerning the form which the displacements u and w must take. This will be considered in a subsequent section.

VI. THE RITZ METHOD AS AN APPROXIMATION TO THE PRINCIPLE OF POTENTIAL ENERGY

Before proceeding to the algebraic formulation of the Rayleigh-Ritz method, it might be well to point out a relationship between the real tire and the assumed toroidal shell. The real tire has finite thickness made up of the carcass and tread regions. Practically all the membrane stiffness of the tire comes about due to the stiffness of the carcass, because the presence of internal pressure generally tends to load all cords into a state of tension where their modulus is high and the surrounding rubber is soft by comparison. Further, this means that essentially all membrane loads are carried by the carcass itself. One might very logically, then, assume that insofar as membrane forces are concerned, the tread is not important to the process of inflation of the tire.

Bending characteristics of the carcass of the tire are reasonably well known from previous work on bending by this group, but it is not possible to make any blanket statements concerning the influence of the tread rubber on bending stiffness since many geometries of design are possible. However, with pure inflation of the tire there will be little circumferential bending. This means that any stiffness of the tread in the circumferential, or tread, directions will not be important to the problem. However, there will be bending in the meridional direction, and this should be taken into account in determining the stiffness of the structure in that direction. It appears that almost all aircraft tires now in manufacture utilize tread cuts in the circumferential direction. This means that the meridional stiffness due to the tread is essentially destroyed since the number of these cuts is generally quite large. Simple experiments with cross sections of tires seem to confirm this line of reasoning. Thus it will be presumed in this study that the carcass of the

tire is the element which carries membrane loads and also provides all the bending stiffness. Furthermore, it is necessary to choose some geometric line as representing the shape of the tire so that the various radii of curvature may be computed from this line; thin shell theory is based on the assumption that the thickness of the shell is very small compared to the dimensions in any other direction, and that this thickness is neglected in determining radii of curvature and other dimensional characteristics. In effect, the shell is treated as a surface with finite membrane and bending rigidity. For the calculations which follow, the midline of the tire carcass will be considered as the geometric line defining the shape of the tire. On this geometric line will be based all the radii of curvature and all the measurements of the various tires treated as shells which follow.

To return to the problem of adapting Eqs. (22) and (30) for solution by the Rayleigh-Ritz method, it is necessary to assume displacement functions u and w which form a complete set and which at the same time automatically satisfy the boundary conditions of the problem. The boundary conditions for a tire under inflation may be listed below.

$$\begin{array}{ll}
 u = u(\alpha) & w = w(\alpha) \\
 u(0) = 0 & \frac{\partial w(0)}{\partial \alpha} = 0 \\
 u(\alpha_r) = 0 & w(\alpha_r) = 0 \\
 u(-\alpha_r) = 0 & w(-\alpha_r) = 0
 \end{array} \tag{31}$$

If one assumes that u and v may be represented by Fourier series, and if one applies the boundary conditions of (31) to the general Fourier series representation of both of the functions u and w , it may be shown that these func-

tions reduce to the following form:

$$\begin{aligned}
 u &= \sum_{n=1} a_n \sin \frac{n\pi\alpha}{\alpha_r} = a_n \bar{u}_n * \\
 w &= \sum_{n=1} b_n \left[\cos \left(\frac{n\pi\alpha}{\alpha_r} \right) - (-1)^n \right] = b_n \bar{w}_n
 \end{aligned}
 \tag{32}$$

Equations (32) may be substituted into the various expressions for strain and for changes in curvature such as given by Eqs. (7), (8) and (13). These give

$$\begin{aligned}
 \epsilon_\phi &= \frac{1}{r_1} (a_n \bar{u}_n' + b_n \bar{w}_n) ** \\
 \epsilon_\theta &= \frac{r_0'}{r_0 r_1} \cdot a_n \bar{u}_n + \frac{b_n \bar{w}_n}{r_2} \\
 -k_\phi &= \frac{1}{r_1^2} \left\{ a_n \bar{u}_n \cdot \frac{r_1'}{r_1} - \frac{r_1'}{r_1} b_n \bar{w}_n' + b_n \bar{w}_n'' + b_n \bar{w}_n \right\} \\
 -k_\theta &= \left\{ -\frac{a_n \bar{u}_n}{r_0 r_1} \left(1 - \frac{r_1}{r_2} \right) \cos \phi + \frac{b_n \bar{w}_n}{r_2^2} + \frac{b_n \bar{w}_n' \cos \alpha}{r_0 r_1} \right\}
 \end{aligned}
 \tag{33}$$

One must now form the following products and squares:

- (a) ϵ_ϕ^2
- (b) ϵ_θ^2
- (c) $\epsilon_\phi \epsilon_\theta$
- (d) $k_\phi \epsilon_\phi$
- (e) $k_\phi \epsilon_\theta$
- (f) $k_\theta \epsilon_\phi$
- (g) $k_\theta \epsilon_\theta$
- (h) k_ϕ^2
- (i) k_θ^2
- (j) $k_\theta k_\phi$

*A repeated subscript will be used as the summation convention.

**A prime denotes $\frac{\partial}{\partial \phi} = \frac{\partial}{\partial \alpha}$.

Working these out is a rather lengthy algebraic job. It will not be repeated here since it is not necessary for the argument being put forth. Now it will be possible to form the strain-energy function as given by Eq. (22) in terms of the displacements u and w . The integral of this function over the surface of the axisymmetric toroidal shell will be designated as U ,

$$U = \int_{-\alpha_r}^{\alpha_r} \Pi \cdot 2\pi r_1 r_0 d\alpha \quad (34)$$

where the coordinates and angles are defined by Fig. 2. Turning now to Eq. (30), the work done during inflation of the tire by the internal pressure may also be expressed in terms of u and w , and hence in terms of the unknown coefficients a_n and b_n . Upon substitution of Eqs. (32) into Eqs. (30), the work done becomes

$$\begin{aligned} W = & 2\pi p \int_{-\alpha_r}^{\alpha_r} \left\{ r_0 r_1 b_n \bar{w}_n + b_n \bar{w}_n b_j \bar{w}_j \left[r_0 + r_1 \cos \alpha \right] \right. \\ & + b_n \bar{w}_n b_j \bar{w}_j r_0 - a_n \bar{u}_n b_k \bar{w}_k \left(r_1 \sin \alpha - \frac{r_1 r_0}{r_1} \right) \\ & \left. - \frac{r_0 r_1}{r_1} b_j \bar{w}_j b_n \bar{w}_n \right\} d\alpha \end{aligned} \quad (35)$$

Forming the potential energy

$$U - W$$

it may be seen that this function depends now on the unknown coefficients a_n and b_n . A set of simultaneous linear equations is obtained by minimizing the value of this function with respect to a_n and b_n . For this purpose, the following equations are needed.

$$\begin{aligned} \frac{\partial}{\partial a_s} (U-W) &= 0 & s = 1, 2, \dots, n \\ \frac{\partial}{\partial b_s} (U-W) &= 0 & s = 1, 2, \dots, n \end{aligned} \quad (36)$$

The actual algebraic manipulations of these equations is a lengthy process

which, for conciseness, will not be repeated here. However, after doing it, it becomes clear that the general type of equation obtained from the system given in Eqs. (43) takes the following form:

$$\sum a_n \int_{\text{Area}} (F1)_n dA + \sum b_n \int_{\text{Area}} (F2)_n dA = 0 \quad (37)$$

$$\sum a_n \int_{\text{Area}} (F2)_n dA + \sum b_n \int_{\text{Area}} (F4)_n dA = \int_{\text{Area}} (F5)_n dA$$

where the functions F1, F2, F4, and F5 are reasonably lengthy algebraic expressions which will be given shortly. The meaning of Eqs. (37) is simply that, having decided upon the number of coefficients n to be retained in expressing u and w, the simultaneous set of Eqs. (37) may be generated by using that number to truncate the series forming the various quadrants of the matrix of simultaneous algebraic equations. The upper half of the right-hand side of this matrix is always zero while the lower half takes on the value $\int (F5)_n dA$. For purposes of various studies made on the influence of these F functions on the solutions, they were originally decomposed into portions arising from various sources. For convenience, they are listed here in that fashion. The membrane contribution to the various F functions arises due to strain energy stored in the membrane itself due to change in area. The bending contribution to strain energy comes about due to bending in both the meridional and circumferential directions during inflation of the tire. The various portions of these F functions are given in Table I so that they may be identified as to source. The contributions labeled "non-linear" arise due to the inclusion in this analysis of second-order terms in the work expression given by Eq. (35), where the final geometry is used as described in Eq. (29). Finally, F5 represents the lower half of the right-hand side of the matrix of simultaneous equations.

TABLE I

'F' FUNCTIONS FOR SIMULTANEOUS EQUATIONS IN COEFFICIENTS a_n AND b_n

F1	Membrane	$2\pi r_0 r_1 (h) \left[E_0 \frac{\bar{u}_k \bar{u}_s}{r_1^2} + \bar{E}_0 \left(\frac{r_0}{r_0 r_1} \right)^2 \bar{u}_k \bar{u}_s + \frac{\bar{F} r_0}{r_0 r_1^2} (\bar{u}_k \bar{u}_s + \bar{u}_k \bar{u}_s) \right]$
	Bending	$2\pi \left(\frac{h^3}{12} \right) \cos \alpha \left[\bar{E}_0 \frac{\bar{u}_k \bar{u}_s}{r_1^2} + \bar{E}_0 \left(\frac{r_0}{r_0 r_1} \right)^2 \bar{u}_k \bar{u}_s + \frac{\bar{F} r_0}{r_0 r_1^2} (\bar{u}_k \bar{u}_s + \bar{u}_k \bar{u}_s) \right]$ $+ 2\pi r_0 r_1 \left[\frac{h^3}{12} \left\{ \bar{u}_k \bar{u}_s \left[\frac{r_1}{r_1} \right]^2 + \frac{E_0 \sin^2 \alpha}{r_0^2 r_1^2} \left(1 - \frac{r_1}{r_2} \right)^2 + \frac{2\bar{F} r_0 \sin \alpha}{r_0 r_1} \left(1 - \frac{r_1}{r_2} \right) \right. \right.$ $\left. \left. - \frac{2\bar{F} r_0 r_1}{r_0^2 r_1 r_2} - \bar{E}_0 \frac{2r_0^2 \sin \alpha}{r_0^2 r_1} \left(1 - \frac{r_1}{r_2} \right) \right\} + (\bar{u}_k \bar{u}_s + \bar{u}_k \bar{u}_s) \left[- \frac{\bar{F} \sin \alpha}{r_0 r_1} \left(1 - \frac{r_1}{r_2} \right) - \frac{r_1}{r_1 r_2} \bar{E}_0 \right] \right]$
	Non-Linear	None
F2	Membrane	$2\pi r_0 r_1 (h) \left[\bar{v}_k \bar{v}_s \left(\frac{r_0}{r_0 r_1} \right) \left(\frac{\bar{E}_0}{r_2} + \frac{\bar{F}}{r_1} \right) + \bar{v}_k \bar{v}_s \left(\frac{1}{r_1} \right) \left(\frac{\bar{E}_0}{r_1} + \frac{\bar{F}}{r_2} \right) \right]$
	Bending	$2\pi \left[\frac{h^3}{12} \right] \cos \alpha \left\{ \bar{v}_k \bar{v}_s \left(\frac{r_0}{r_0 r_1} \right) \left(\frac{\bar{E}_0}{r_2} + \frac{\bar{F}}{r_1} \right) + \bar{v}_k \bar{v}_s \left(\frac{1}{r_1} \right) \left(\frac{\bar{E}_0}{r_1} + \frac{\bar{F}}{r_2} \right) \right\}$ $+ 2\pi r_0 r_1 \left[\frac{h^3}{12} \right] \left\{ \bar{v}_k \bar{v}_s \left[\frac{r_1}{r_1} \left(1 - \frac{r_1}{r_2} \right) \bar{E}_0 - \frac{E_0 \sin \alpha}{r_0^2 r_1 r_2} \left(1 - \frac{r_1}{r_2} \right)^2 - \frac{r_0}{r_0^2 r_1 r_2} \left(\bar{F} + \frac{r_1}{r_2} \bar{E}_0 \right) \right] \right.$ $+ \bar{v}_k \bar{v}_s \left[- \frac{1}{r_1^2} \left(\bar{E}_0 \frac{r_1^2}{r_1^2} - \frac{\bar{F} r_0 r_1}{r_0 r_1} \right) - \frac{\bar{F} r_0 \sin \alpha}{r_0 r_1} \left(2 - \frac{r_1}{r_2} \right) + \bar{E}_0 \frac{r_0 \sin \alpha}{r_0^2 r_1} - \bar{E}_0 \frac{\sin^2 \alpha}{r_0^2 r_1} \left(1 - \frac{r_1}{r_2} \right) \right]$ $+ \bar{v}_k \bar{v}_s \left[\frac{\bar{E}_0}{r_1^2} \left(\frac{r_1}{r_1} \right) + \frac{\bar{F}}{r_0 r_1} \sin \alpha \right] - \bar{v}_k \bar{v}_s \left(\frac{1}{r_1 r_2} \right) \left(\bar{E}_0 + \frac{\bar{F} r_1}{r_2} \right)$ $+ \bar{v}_k \bar{v}_s \left(\frac{1}{r_1} \right) \left(\bar{E}_0 \frac{r_1}{r_2} + \frac{\bar{F} r_0 \sin \alpha}{r_0} \right) - \bar{v}_k \bar{v}_s \left(\frac{\bar{E}_0}{r_1 r_2} \right) \left. \right\}$
	Non-Linear	$2\pi p \cdot \bar{v}_k \bar{v}_s \left(r_1 \sin \alpha - \frac{r_1 r_0}{r_1} \right)$
F4	Membrane	$2\pi r_0 r_1 (h) \bar{w}_k \bar{w}_s \left(\frac{\bar{E}_0}{r_1} + \frac{\bar{E}_0}{r_2} + \frac{2\bar{F}}{r_1 r_2} \right)$
	Bending	$2\pi \left(\frac{h^3}{12} \right) \cos \alpha \left[\bar{w}_k \bar{w}_s \left(\frac{\bar{E}_0}{r_1} + \frac{\bar{E}_0}{r_2} + \frac{2\bar{F}}{r_1 r_2} \right) \right]$ $+ 2\pi r_0 r_1 \left[\frac{h^3}{12} \right] \left\{ \bar{w}_k \bar{w}_s \left[\frac{\bar{E}_0}{r_1} + \frac{\bar{E}_0}{r_2} - \frac{2}{r_1 r_2} \left(\frac{\bar{E}_0}{r_1} + \frac{\bar{E}_0}{r_2} + \frac{\bar{F}}{r_1 r_2} \right) \right] \right.$ $+ \bar{w}_k \bar{w}_s \left(1 - \frac{r_1}{r_2} \right) \left(\bar{E}_0 \frac{\sin \alpha}{r_0^2 r_1 r_2} - \bar{E}_0 \frac{r_1}{r_1^2} \right) + \bar{w}_k \bar{w}_s \left(\frac{1}{r_1} \right) \left(1 - \frac{r_1}{r_2} \right) \bar{E}_0$ $+ \bar{w}_k \bar{w}_s \left(1 - \frac{r_1}{r_2} \right) \left(\bar{E}_0 \frac{\sin \alpha}{r_0^2 r_1 r_2} - \bar{E}_0 \frac{r_1}{r_1^2} \right) + \bar{w}_k \bar{w}_s \left[\frac{\bar{E}_0}{r_1^2} \left(\frac{r_1}{r_1} \right)^2 + \bar{E}_0 \frac{\sin^2 \alpha}{r_0^2 r_1} + \frac{2\bar{F} r_0 \sin \alpha}{r_0 r_1} \right]$ $- \bar{w}_k \bar{w}_s \left[\frac{\bar{E}_0}{r_1^2} \left(\frac{r_1}{r_1} \right) + \frac{\bar{F} \sin \alpha}{r_0 r_1} \right] + \bar{w}_k \bar{w}_s \left(\frac{1}{r_1} \right) \left(\bar{E}_0 - \frac{r_1}{r_2} \bar{E}_0 \right)$ $- \bar{w}_k \bar{w}_s \left(\frac{1}{r_1} \right) \left(\bar{E}_0 \frac{r_1}{r_1} + \frac{\bar{F} r_0 \sin \alpha}{r_0} \right) + \bar{w}_k \bar{w}_s \left(\frac{\bar{E}_0}{r_1} \right) \left. \right\}$
	Non-Linear	$- 2\pi p \left\{ 2\bar{w}_k \bar{w}_s \left[r_0 + r_1 \cos \alpha \right] + r_0 \left(\bar{w}_k \bar{w}_s + \bar{w}_k \bar{w}_s \right) - \frac{r_0 r_1}{r_1} \left(\bar{w}_k \bar{w}_s + \bar{w}_k \bar{w}_s \right) \right\}$
F5		$2\pi r_0 r_1 \bar{v}_s$

VII. SUMMARY OF STUDIES ON THE ELASTIC NATURE OF CORD-RUBBER LAMINATES

Equations (17) and (18) indicate that the strain energy at any point on the surface of the tire can be written only if the orthotropic elastic constants \bar{E}_ϕ , \bar{E}_θ and \bar{F} are known at that point. This means that some mechanism must be found for determining these elastic constants at any position on the meridian of the tire, since they are, due to the method of manufacturing, axisymmetric. Using the angle α as a variable, one might say that each of these three elastic constants are functions of the angle α , as shown in Fig. 2.

The author has shown that the elastic constants of a sheet made up of laminated plies could be calculated quite easily in the directions of the bisectors of the angles of the cords, these directions being the principal directions of elasticity. The methods presented in these references required a knowledge of the basic constants of a single sheet of the laminate, these latter constants being denoted by E_x , E_y , F_{xy} , and G_{xy} . Using these references, it is seen that all necessary elastic constants may be determined provided that the basic constants are known and provided that the cord angle is known. A technical report recently issued by this group²⁰ shows that approximate expressions may be developed for calculating E_x , E_y , F_{xy} , and G_{xy} if the materials and geometry making up each individual ply are known. When this information is given, then all elastic constants may be calculated if the local cord angle is known.

Consider any point on the carcass centerline of the meridional cross section of the tire as defined by the angle which the normal makes with a vertical, called in this report α . At this angle α there exists some local cord angle which, if the materials and geometry of each ply are known as well as the number of plies, determines completely the elastic constants at that point.

A straightforward method of determining the local cord angle at this point was given earlier in this report as Eq. (1) under conditions of inextensibility of the cords. During forming of the tire, extension of the cords is known to take place and for that reason different types of correction expressions have often been applied to Eq. (1). An alternate approach to this process is to use Eq. (1) in a slightly different form in which extensibility of the cords is much less important. Evidence on this point has been furnished and will be used here to justify the process. Figure 2 illustrates the notation that the maximum radius to the crown of the tire may be denoted by r_{OC} , and calling the cord angle at the crown of the formed tire β_C , an expression may be derived similar to Eq. (1) but now involving the crown as a base point rather than the rim. This gives

$$\cos \beta = \frac{r_O}{r_{OC}} \cos \beta_C \quad (38)$$

where β represents, as before, the local cord angle. Table II represents data taken from measurements on X-ray photographs of an actual tire at various radii r_O . Calculated values of the angle β using Eq. (38) are also presented. Over most of the tire the agreement is quite good, although Eq. (38) uses no correction factors for cord extension. By use of Eq. (38) it should be possible to calculate accurately the cord angle at most places on the meridian of the cross section of the tire, once the crown cord angle and crown radius, measured to the midline of the carcass, are given. The complete nature of the distribution of elastic constants around the meridian of the tire may then be determined if the properties of the materials and geometry of construction in a single ply are given.

The concepts outlined here allow complete specification of the elastic constants and do so in a fashion capable of being programmed digitally as part of the larger, over-all tire program.

TABLE II

COMPARISON BETWEEN MEASURED AND CALCULATED CORD ANGLES

Radius r_o	Cord angle measured from X-ray photographs	Cord angle calculated from Eq. (38)
$r_{oc} = 23.57$	Crown cord angle = 38.5	---
22.43	41	41.75
19.43	50	49.65
16.93 (rim)	52	55.65

VIII. INTERNAL STRESS ANALYSIS OF THE TOROIDAL SHELL
UNDER INTERNAL PRESSURE

The tire under internal pressure poses a particularly appropriate problem with which to begin this series of efforts to analyze tires under various loading conditions using digital computation techniques. This is because, as mentioned previously, the primary consideration in this problem is that of membrane effects, and further, that these result in tensile cord loads throughout the structure. This means that it will not be necessary to account for the sudden change in modulus as the cord load goes from tension to compression.

Discussions with research sponsors indicate that present practice is to design tires so that, upon inflation, bending effects are either small or negligible. For this reason, it is anticipated that in most problems of interest cord loads contributed by bending effects during the inflation process alone will be negligible compared to cord loads generated by membrane forces. Using this simplification, it is possible to calculate the deformation state of the tire using both membrane and bending effects, and to use those effects in a very simple and straightforward way to obtain the two quantities of structural interest here, the cord loads and interply stresses.

Turning first to cord loads, it may be seen from work done by the author²³ that cord loads may be determined completely if the thickness of each ply, the end count, and the stress distributions all are known, from the equation

$$P = \frac{h}{n} \left[(L) \sigma_{\theta} + (M) \sigma_{\phi} \right] \quad (39)$$

where

h = thickness of a single ply

n = end count

L, M = coefficients given from Ref. 23

σ_{θ} , σ_{ϕ} = membrane stresses as given from shell analysis

Equation (39) is adapted to the axisymmetric case of loading by internal pressure where no shearing stresses are present in the structure.

The calculation of interply stresses is a relatively straightforward process throughout the tire if one considers only the effect of membrane forces. The previous discussion indicated that these would be predominant and, for purposes of this program, will be the only ones considered here. From Refs. 24 and 25, it may be seen that the interply stresses for cases of membrane forces induced in the carcass are given by

$$\sigma_{\phi\theta}'' = h \left[- \frac{a_{13}(+\alpha)}{a_{33}(+\alpha)} \sigma_{\theta} - \frac{a_{23}(+\alpha)}{a_{33}(+\alpha)} \sigma_{\phi} \right] \quad (40)$$

where the functions $a_{13}(+\alpha)/a_{33}(+\alpha)$ and $a_{23}(+\alpha)/a_{33}(+\alpha)$ are given in Ref. 24 as functions of the elastic characteristics of the system and of the cord angle α . The stresses σ_{θ} and σ_{ϕ} may be determined from the deformation analysis of the tire. With these, and with a knowledge of the elastic characteristics around the meridian, interply stresses as given by Eqs. (40) may be obtained at once.

The digital computer program presented in this report utilizes cord loads and interply stresses determined only from membrane effects, as discussed in this section of the report. More complete analyses, including the effect of bending on cord loads and interply stresses, can be included by revision of only a small portion of the total digital computer program. This will not be attempted here since it is rather lengthy and would not be of wide interest.

IX. DIGITAL COMPUTER PROGRAM FOR CORD LOADS, INTERPLY STRESSES, AND DEFORMATIONS DUE TO INFLATION

The computer program was written to perform the task of producing the system of Eqs. (37), solving them, and consequently obtaining the desired results as output. The details of the program will not help to understand the problem, but a few words about its broad structure will allow a potential user a view of the procedure and will show how it can be adapted to his particular needs.

The program consists of a "main" or controlling program, which is very short, and calls upon a number of subprograms or subroutines. Such a procedure has been followed throughout this project inasmuch as it permits checking discrete parts easily or even altering them as situations dictate. The program required reading in data of basic material properties and certain control parameters, such as the number of terms of the Fourier expansion which are to be used in the Ritz procedure. The radii of curvature may be imbedded, as a table, in the program, or alternately this information may also be read in as data at the discretion of the programmer.

The list of subroutines which are used will give an approximate outline of the computing sequence. These are in turn controlled by the main program.

Subroutines

1. Data reading.
2. Raw material properties preparation.
3. Preparation of a table of material properties as a function of position on the tire.
4. A utility routine which prepares certain parameters appearing frequently in the subsequent computation.

5. Ritz procedure, which in turn requires
 - (a) Simpson's rule procedure, which further needs
 - (i) a procedure for evaluating the arguments of the integrals for the evaluation of the augmented coefficient matrix of Eqs. (37);
 - (ii) tables for radii of curvature and material properties;
 - (iii) Subroutine for displacements and their derivatives.
 - (b) Simultaneous equation solver.
6. Final results are produced after the computation of the coefficients of the Fourier expansion for the displacements.

Depending on the nature of the input parameters, it is possible, for a given set of material properties, to compute the results repeatedly using an increasing number of terms in the Fourier expansion. This is accomplished by cycling over subroutines 5 and 6 repeatedly.

The computations in subroutine 5 are very extensive, and efforts have been made to make this part of the computation as economical as possible. It is anticipated that in future programs even greater efforts will have to be exerted in this direction; however, much of what can be done here depends on the size of the machine memory available.

X. EXAMPLE ANALYSIS

The principal objective of this report is to illustrate a typical strength analysis of an aircraft tire under internal pressure. This is considerably more important in aircraft tires than in other tires due to the fact that their pressure loadings are generally much greater. For purposes of this analysis, a 32 x 8.8, Type VII, aircraft tire was obtained on loan from one of the major aircraft tire manufacturers, along with a standard wheel for this tire. Here the particular tire obtained was a nominal twelve ply rating tire manufactured for a special use and hence was slightly lighter than the usual 32 x 8.8 design. It actually contained six plies of carcass material. As an anti-skid device, its tread stock was loaded with wire in a random dispersion but that factor did not influence the subsequent inflation calculations.

Plaster casts were made of both the inner and outer surfaces of the tire and from these casts, along with complete information on the carcass thickness furnished by the manufacturer, it was possible to produce a drawing of the carcass midline of the tire. It was then necessary to use this carcass midline to determine the radii of curvature at various points around the meridian, or crosssection, of the tire.

In connection with tire analysis work during the past two years, a problem has arisen several times in determining radii of curvature of an irregular shape which is drawn out on a piece of paper. At various times different schemes have been used for actually calculating these radii of curvature, and such schemes have embraced ideas involving:

(a) the use of mechanical systems such as dial gauges to produce numerical data which in turn could be differentiated and treated numerically by a

digital computer program.

(b) drawing out the cross-section on a piece of graph paper from which hand calculations on a desk computer can give radii of curvature.

(c) fitting a polynomial to the shape of the tire and from this polynomial determining radii of curvature, curve fitting being done by a least squares approach on a digital computer.

(d) an optical method which determines the normal to the curve at any point, and from which radii of curvature may be obtained by one graphical differentiation.

None of these systems appears to be completely satisfactory, and our current impression is that a great deal of the difficulty lies in the absence of a good smoothing routine which can be used with the digital computer. The problem is one which is annoying but not serious, and, for this particular example analysis, the first and last of these methods were used separately and reworked carefully until the results seemed to agree.

Through the kindness of the B. F. Goodrich Research Laboratories, which furnished this particular aircraft tire, complete data was obtained on the characteristics of the material used in the tire, as well as information on tire geometry and construction details. This enabled all necessary input data for the analysis to be obtained directly. Fig. 6 shows reproductions of the digital printout pages; the first page illustrates the input data and shows the values of rubber modulus, the various cord properties, the number of plies, cord count, and crown angle. For this particular 12 ply rated tire the recommended inflation pressure is 95 psi and this value is used as input. The maximum number of Ritz terms in the solution is taken to be eight and from this the digital computations may proceed.

The second page of Fig. 6 illustrates elastic constants which are calculated at various stations I, where I = 1 refers to an angle $\alpha = 0$, this

TIRE INFLATION PROGRAM

INPUT DATA

RAN MATERIAL PROPERTIES

RUBBER PROPERTIES

YOUNG'S MODULUS = 450 PSI.
SHEAR MODULUS = 150 PSI.
POISSON RATIO = .500

STRUCTURE PROPERTIES

NUMBER OF PLYS = 6
PLY THICKNESS = .031 IN.
CORD COUNT = 33
CROWN ANGLE = 34.0 DEG.

INFLATION PRESSURE = 95.00 PSI.

GEOMETRIC DATA

ALPHA = LOCATION ANGLE
R0 = PRINCIPLE RADIUS IN THETA PLANE
R1 = PRINCIPLE RADIUS IN PHI PLANE
RIP = DERIVATIVE OF RADIUS IN PHI PLANE

CORD PROPERTIES

AESUBC = 75 LBS.
SHEAR MODULUS = 700 PSI.
POISSON RATIO = .700
DIAMETER = .021 IN.

(AESUBC = SPRING CONSTANT TIMES LENGTH)

PROGRAM CONTROLS

LIMIT OF INTEGRATION = 2.10270 RAD.
SENSITIVITY FACTOR = 8
NUMBER OF DATA STATIONS = 32
MINIMUM NUMBER OF RITZ TERMS = 5
MAXIMUM NUMBER OF RITZ TERMS = 8
LIMIT OF COMPUTATION = 2.10300 RAD.

Fig. 6. Input and output pages of digital computer program.

I I R E I N F L A T I O N P R O G R A M

CUIPUT DATA

I	ALPHA	ETH-BAR	EPHI-BAR	F-BAR	X-COOD.	Y-COOD.	KO	KI	RIP
1	4.5	38232.1	9341.3	18043.8	-0.00	4.732	14.000	7.000	2.200
2	9.0	37421.1	9781.7	18107.3	-0.584	4.707	13.950	7.900	-0.230
3	12.5	36247.5	10152.5	18285.8	-1.201	4.634	13.890	7.950	-0.720
4	16.0	34879.5	10618.2	18405.7	-1.650	4.550	13.800	7.000	-2.350
5	20.0	33810.9	11009.2	18497.1	-2.036	4.434	13.690	6.050	-2.350
6	24.0	32450.9	11544.4	18609.8	-2.405	4.334	13.600	5.050	-2.350
7	28.5	31583.0	11909.8	18679.2	-2.701	4.216	13.480	4.100	-2.350
8	34.0	29342.6	12949.5	18847.7	-2.957	4.091	13.400	3.150	-1.300
9	40.5	27654.0	13837.8	18961.8	-3.189	3.952	13.180	2.500	-0.840
10	47.5	25746.5	14969.1	19074.0	-3.397	3.796	13.000	2.100	-0.700
11	54.5	24300.8	15932.0	19144.6	-3.569	3.631	12.780	1.800	-0.440
12	61.5	22659.8	17154.5	19206.2	-3.709	3.459	12.600	1.650	-0.250
13	67.5	21410.8	18192.4	19237.4	-3.808	3.300	12.380	1.600	-0.100
14	74.0	19988.1	19507.8	19253.3	-3.880	3.149	12.200	1.600	-0.100
15	80.0	18902.0	20622.9	19249.0	-3.941	2.972	11.980	1.700	-0.230
16	85.5	17661.7	22034.3	19223.6	-3.982	2.791	11.800	1.850	-0.400
17	90.5	16712.9	23229.7	19187.2	-4.006	2.604	11.580	2.100	-0.550
18	95.0	15627.6	24741.9	19124.5	-4.012	2.410	11.400	2.350	-0.730
19	99.5	14756.3	26022.3	19059.1	-4.002	2.214	11.180	2.650	-0.800
20	103.5	13844.7	27641.5	18962.6	-3.974	1.992	11.000	3.050	-1.110
21	107.0	13115.6	29012.4	18870.9	-3.928	1.768	10.780	3.500	-1.500
22	110.0	12354.3	30586.2	18756.3	-3.866	1.544	10.600	4.100	-2.000
23	112.5	11573.0	32381.2	18615.4	-3.792	1.324	10.400	4.800	-2.600
24	115.0	10974.9	33902.0	18489.4	-3.709	1.111	10.180	5.700	-3.200
25	116.5	10251.7	35827.3	18323.0	-3.599	0.862	10.000	6.750	-3.900
26	118.0	9769.9	37459.7	18177.3	-3.514	0.687	9.780	8.100	-4.500
27	119.0	9227.7	39336.9	18006.1	-3.407	0.480	9.600	9.700	-5.100
28	119.5	8723.5	41284.4	17825.9	-3.319	0.318	9.400	11.500	-5.700
29	119.5	8211.3	43512.5	17618.2	-3.266	0.223	9.200	13.300	-6.300
30	120.0	7824.3	45406.5	17441.8	-3.205	0.116	8.980	15.000	-6.900
31	120.3	7389.7	47813.8	17219.4	-3.165	0.048	8.800	16.000	-7.500
32	120.5				-3.137	-0.000	8.580	16.000	-8.100

Fig. 6 (Continued).

 WIRE INFLATION PROGRAM

STATION	ALPHA	BETA	X-COORD.	Y-COORD.	X-DISPL.	Y-DISPL.	U-DISPL.	W-DISPL.
1	34.0	-0.000	5.277	-0.000	.5449	.0000	.5449	.0000
2	4.5	-.636	5.247	-.0526	.5392	.0102	.5417	.0102
3	34.3	-1.302	5.157	-.1007	.5225	.0178	.5318	.0178
4	12.5	-1.783	5.053	-.1326	.5025	.0208	.5193	.0208
5	16.0	-2.195	4.930	-.1585	.4776	.0207	.5028	.0207
6	24.0	-2.585	4.779	-.1801	.4448	.0171	.4796	.0171
7	37.0	-2.895	4.626	-.1935	.4099	.0101	.4532	.0101
8	28.5	-3.157	4.462	-.2004	.3708	-.0008	.4215	-.0008
9	34.0	-3.389	4.279	-.1996	.3263	-.0170	.3821	-.0170
10	40.5	-3.587	4.075	-.1896	.2797	-.0375	.3358	-.0375
11	47.5	-3.741	3.867	-.1720	.2358	-.0576	.2861	-.0576
12	54.9	-3.860	3.655	-.1513	.1968	-.0740	.2369	-.0740
13	61.5	-3.943	3.470	-.1351	.1698	-.0847	.1998	-.0847
14	67.5	-4.002	3.300	-.1226	.1507	-.0923	.1710	-.0923
15	74.0	-4.051	3.106	-.1098	.1333	-.0978	.1423	-.0978
16	80.0	-4.082	2.910	-.0995	.1183	-.0992	.1186	-.0992
17	85.5	-4.100	2.708	-.0942	.1048	-.0971	.1022	-.0971
18	90.5	-4.105	2.502	-.0932	.0927	-.0935	.0925	-.0935
19	95.0	-4.095	2.296	-.0927	.0819	-.0896	.0853	-.0896
20	99.5	-4.062	2.063	-.0883	.0711	-.0846	.0754	-.0846
21	103.5	-4.006	1.829	-.0882	.0613	-.0778	.0618	-.0778
22	107.0	-3.930	1.597	-.0642	.0523	-.0687	.0462	-.0687
23	110.0	-3.841	1.368	-.0494	.0437	-.0579	.0315	-.0579
24	112.5	-3.745	1.146	-.0361	.0355	-.0466	.0198	-.0466
25	115.0	-3.622	.888	-.0231	.0261	-.0334	.0099	-.0334
26	116.5	-3.530	.707	-.0158	.0198	-.0247	.0054	-.0247
27	118.0	-3.417	.493	-.0092	.0128	-.0157	.0021	-.0157
28	119.0	-3.325	.326	-.0053	.0079	-.0095	.0008	-.0095
29	119.5	-3.269	.228	-.0034	.0053	-.0063	.0003	-.0063
30	120.0	-3.207	.119	-.0016	.0027	-.0031	.0001	-.0031
31	120.3	-3.166	.049	-.0007	.0011	-.0013	.0000	-.0013
32	120.5	-3.137	-.000	-.0000	-.0000	-.0000	.0000	-.0000

Fig. 6 (Continued).

being the crown of the tire. The location associated with the point $I = 32$ is an angle $\alpha = 120.5$ degrees, which is the rim of the tire. The intermediate points are obtained by using increments of 4.50 of the normal angle α . In general these will be slightly unequal arc lengths due to the fact that the radius of curvature r_1 is continuously changing.

The next three columns on the second page of Fig. 6 represent elastic constants in the θ , or circumferential direction of the tire and in the ϕ , or meridional direction of the tire. It is interesting to note the extremely wide variation in elastic constants demonstrated between the crown and the rim of the tire. The column labeled \bar{F} is approximately constant, however, from crown to rim.

In the next two columns the x and y coordinates of the carcass midline are calculated and listed. Finally, the last three columns give the radii r_0 , r_1 , and $\frac{dr_1}{d\alpha}$, which is labeled here RLP. These radii of curvature are necessary for the construction of the strain energy functions described previously.

On the third page of Fig. 6 a portion of the output from this program is given. The first column again indicates the number of the station to which the data pertains, the second column gives the angle of the normal with respect to the vertical center line, the third column gives the calculated cord angle β at each of these positions; the next two columns give the x and y coordinates of the inflated tire, and the columns labeled y displacement and x displacement give the actual displacements of these points. Finally, the displacements normal and tangential to the carcass midline are denoted by the usual notation w and u, and these are listed. This information is sufficient to draw out the final, or inflated, shape of the tire. In the final page, one finds again a station location column followed by a calculation of the membrane strains labeled EPSPHI and EPSTH. Using these values

of membrane strain one may calculate membrane stresses, and these are listed as SIGPHI and SIGTH, standing for σ_ϕ and σ_θ respectively. The next column, labeled INTPLY, gives the interply stresses between plies calculated on a membrane basis. The last column lists the cord loads induced by membrane stresses; from this column it may be seen that the maximum cord load occurs at the crown of the tire. At this point the load is approximately 4 pounds per cord, which appears not unreasonable in light of the known strengths of the typical textile cords used in such tire manufacture.

As a final item, the bead of the tire may be treated as a ring subjected to outwardly directed tensile forces. If this is done, then the total bead force generated by these tensile forces may easily be calculated. In this particular case, the tensile forces arise due to the presence of the stress σ_θ in the tire and the bead forces are worked out as an integral part of this program. In this particular case they turn out to be approximately 1250 pounds, which is well within their strength capabilities.

In viewing the overall results of this computer program, one sees that the maximum cord loads apparently occur in the crown of the tire. This seems to agree with what is generally known about the failure of tires under pure internal pressure, such as a high pressure hydrostatic testing. In those cases it appears, from what evidence is available, that failures initiate at the crown of the tire due to internal pressure alone.

To check the validity of these calculations, the particular aircraft tire used here was inflated to 95 pounds of internal pressure and a complete casting made of the outer surface. By comparing this casting with one previously made of the uninflated tire, one could immediately obtain information on the growth of the tire due to inflation at different positions α . This information can be compared with the final configuration of the tire as given from the calculations, and is done so in Figs. 7a and 7b. From the comparison

of calculated and measured deflections it can be seen that the calculations seem to agree quite well in the crown and sidewall areas of the tire. Some discrepancy exists between measurement and calculations in the shoulder area for which there is no reasonable explanation, at the moment. However, it should be noted that past experience with such calculations indicates that the resulting deflections are quite sensitive to the quality of the radii of curvature which are measured in any particular shell. In view of the fact that the radii of curvature obtained here were compromises, in certain respects, between two different methods of obtaining such data, it might be expected that the use of radii of curvature which were completely correct would perhaps improve the deflection data obtained. It will be necessary to examine this point in some detail at a later time.

A photograph of the tire mounted on the wheel is shown in Figs. 8a and 8b.

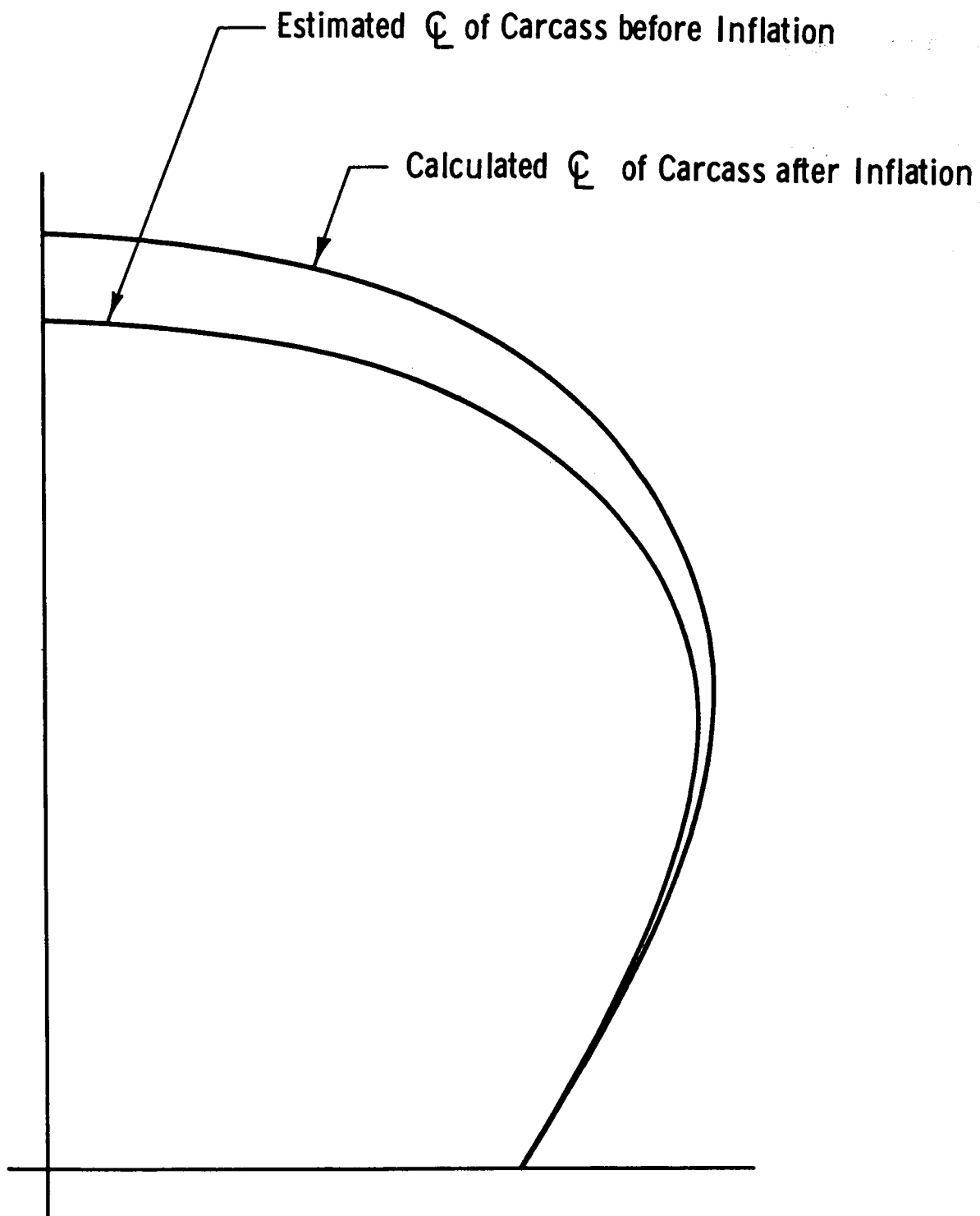


Fig. 7. Comparison of calculated and measured inflated shapes for a 32x8.8 aircraft tire.

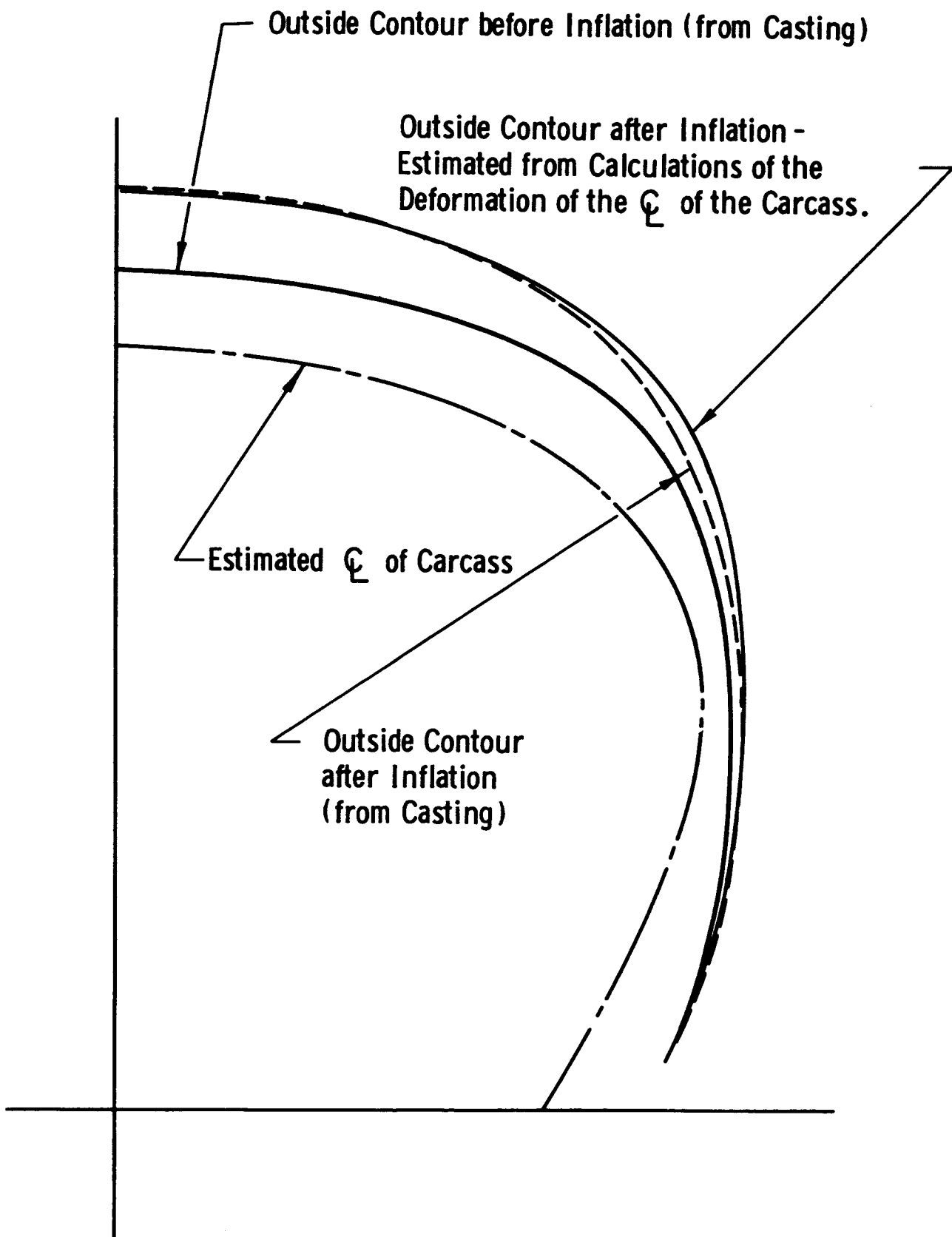


Fig. 7 (Concluded).

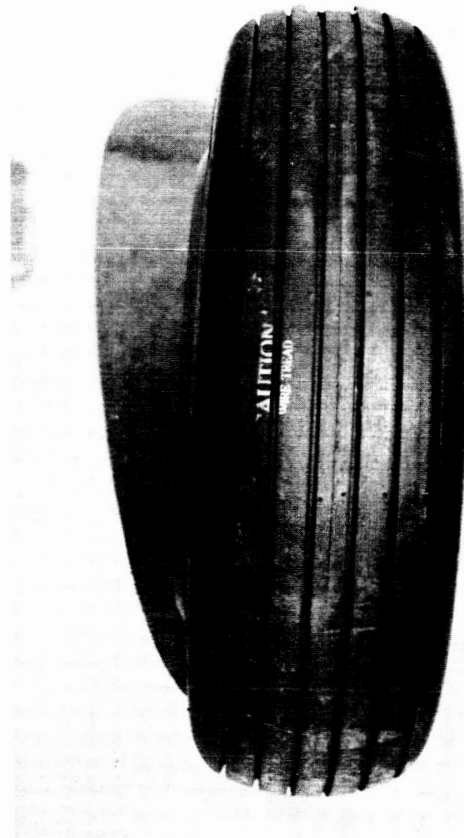
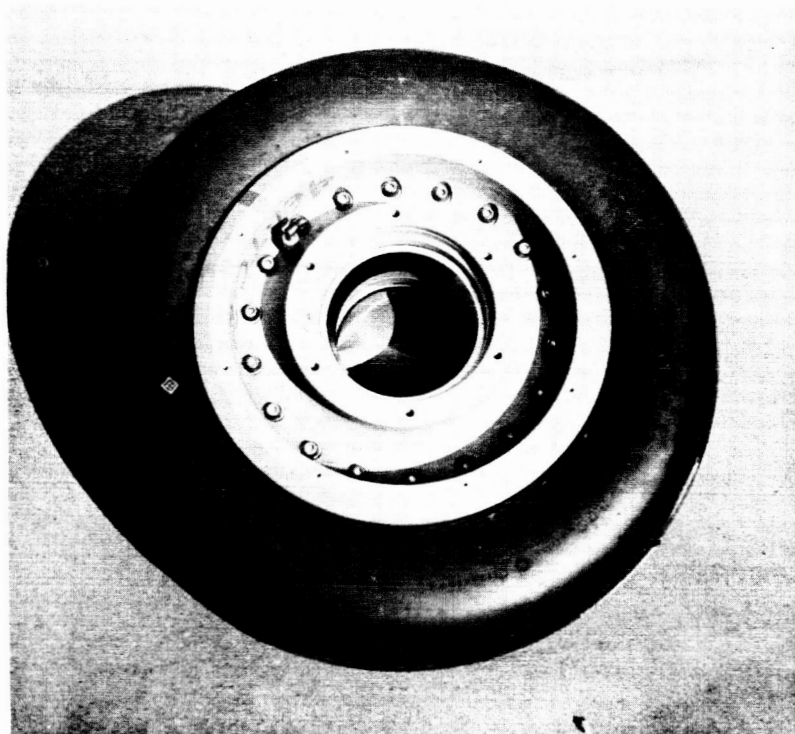


Fig. 8. Photographs of a tire.

ACKNOWLEDGMENTS

The authors of this report would like to acknowledge the co-operation of the B. F. Goodrich Research Laboratories in furnishing the aircraft tire used in the example analysis, and the General Tire and Rubber Co. in furnishing an aircraft wheel upon which the tire could be mounted.



REFERENCES

1. Clark, S. K., "Plane Elastic Characteristics of Orthotropic Laminates," Textile Res. Journ., April 1963.
2. Hadekel, R., "Some Notes on Pneumatic Tires," Aircraft Engineering, 11 (January 1944).
3. Hofferberth, W., "On the Statics of Pneumatic Tires," Kautschuk und Gummi, 8, No. 5. 124WT-130WT.
4. Rotta, J., "Zur Statik Des Luftreifens," Ingenieur-Archiv, 17, 129-141, (1949).
5. Lauterbach, H. G., "Fundamental Tire Studies," 1959 Dupont Tire Yarn Technical Review, 35.
6. Clark, S. K. and Field, N. L., "Simple Approximations for Stresses in a Tire," Univ. of Mich., ORA Report 02957-10-T, Ann Arbor, October 1961.
7. Hadekel, R., The Mechanical Characteristics of Pneumatic Tires, Technical Information Bureau, Ministry of Supply S and T Memo No. 10/52.
8. Timoshenko, S., and Woinowski-Krieger, S., Theory of Plates and Shells, McGraw-Hill Book Co., New York, 1959.
9. Clark, R. A., "On the Theory of Thin Elastic Toroidal Shells," J. Math. and Phys., 19, No. 3, 146 (October, 1950).
10. Kantorovich, L. V., and Krylov, V. I., Approximate Methods of Higher Analysis, Interscience Publishers, Inc., New York, 1958.
11. Novoshilov, V. V., The Theory of Thin Shells, P. Noordhoff, Ltd., Groningen, 1959.
12. Wissler, H., "Festigkeitsberechnung von Ringflächenschalen," doctoral thesis, Zürich, 1916.
13. Dahl, N. C., "Toroidal-Shell Expansion Joints," J. Appl. Mech., 497, (December 1953).
14. Knowles, J. K., and Reissner, E., "A Derivation of the Equations of Shell Theory for General Orthogonal Coordinates," J. Math. and Phys., 35, 351-358 (1957).
15. Knowles, J. K., and Reissner, E., "Note on Stress-Strain Relations for Thin Elastic Shells," J. Math. and Phys., 37, 269-282 (1958).
16. Knowles, J. K., and Reissner, E., "On Stress-Strain Relations and Straine-Energy Expressions in the Theory of Thin Elastic Shells," J. Appl. Mech., 184, (March 1960).

REFERENCES (Concluded)

17. Flugge, W., Stresses in Shells, Springer-Verlag, Berlin, 1960.
18. Wang, C. T., Applied Elasticity, McGraw-Hill Book Co., Inc., New York, 1953.
19. Clark, S. K., and Robbins, D. H., Bending Characteristics of Cord-Rubber Laminates, Univ. of Mich. ORA Report 02957-9-T, Ann Arbor, August, 1961.
20. Clark, S. K., Dodge, R. A., and Field, N. L., Calculation of the Elastic Constants of a Single Sheet of Rubber-Coated Fabric, Univ. of Mich. ORA Report 02957-13-T, Ann Arbor, October 1961.
21. Clark, S. K., The Plane Elastic Characteristics of Cord-Rubber Laminates, Univ. of Mich. ORA Report 02957-3-T, Ann Arbor, October 1960.
22. Clark, S. K., The Elastic Constants of Cord-Rubber Laminates, Univ. of Mich. ORA Report 02957-6-T, Ann Arbor, October, 1960.
23. Clark, S. K., Cord Loads in Cord-Rubber Laminates, Univ. of Mich. ORA Report 02957-5-T, Ann Arbor, October, 1960.
24. Clark, S. K., Interply Shear Stresses in Cord-Rubber Laminates, Univ. of Mich. ORA Report 02957-4-T, Ann Arbor, October 1960.
25. Dodge, R. N., Field, N. L., and Clark, S. K., The Plane Elastic Characteristics of Cord-Rubber Laminates—II, Univ. of Mich. ORA Report 02957-7-T, Ann Arbor, June 1961.
26. Field, N. L., Coon, M. D., Claus, A. J., and Clark, S. K., The Mechanics of Pneumatic Tires, I. Preliminary Investigations and Experiments, Univ. of Mich. ORA Report 02957-1-D, Ann Arbor, March 1960.